
Your Absorbing Discrete Diffusion Secretly Models the Conditional Distributions of Clean Data

Jingyang Ou¹ Shen Nie¹ Kaiwen Xue¹ Fengqi Zhu¹
 Jiacheng Sun² Zhenguo Li² Chongxuan Li^{1*}

¹Gaoling School of Artificial Intelligence, Renmin University of China

²Huawei Noah's Ark Lab

{oujingyang, nieshen, kaiwenxue, chongxuanli}@ruc.edu.cn;
 fengqizhu@whu.edu.cn; {sunjiacheng1, li.zhenguo}@huawei.com;

Abstract

Discrete diffusion models with absorbing processes have shown promise in language modeling. The key quantities to be estimated are the ratios between the marginal probabilities of two transitive states at all timesteps, called the concrete score. In this paper, we reveal that the concrete score in absorbing diffusion can be expressed as conditional probabilities of clean data, multiplied by a time-dependent scalar in an analytic form. Motivated by this finding, we propose reparameterized absorbing discrete diffusion (RADD), a dedicated diffusion model without time-condition that characterizes the time-independent conditional probabilities. Besides its simplicity, RADD can reduce the number of function evaluations (NFEs) by caching the output of the time-independent network when the noisy sample remains unchanged in a sampling interval. Empirically, RADD is up to 3.5 times faster while achieving similar performance with the strongest baseline. Built upon the new perspective of conditional distributions, we further unify absorbing discrete diffusion and any-order autoregressive models (AO-ARMs), showing that the upper bound on the negative log-likelihood for the diffusion model can be interpreted as an expected negative log-likelihood for AO-ARMs. Further, our RADD models achieve SOTA performance among diffusion models on 5 zero-shot language modeling benchmarks (measured by perplexity) at the GPT-2 scale. Our code is available at <https://github.com/ML-GSAI/RADD>.

1 Introduction

Auto-regressive models [1, 2, 3] have dominated the area of language modeling for many years. In particular, such models significantly benefit from large-scale transformers [4] and training data and have achieved remarkable progress [5, 6, 7, 8]. From a probabilistic perspective, the sequential sampling process of auto-regressive models is inefficient and limits the reasoning ability in nonsequential orders [9, 10]. Intrinsically, this is because such models characterize the joint distribution by the chain rule of probability, motivating research on developing other types of generative models for text.

Diffusion models [11, 12, 13] generate data in a coarse-to-fine manner efficiently [14, 15, 16, 17, 18] and all dimensions simultaneously, providing an appealing alternative to auto-regressive models. Among other efforts [19, 20, 21, 22, 23, 24, 25, 26, 27, 28, 29] (see Section 5 for a comprehensive discussion), score entropy discrete diffusion (SEDD) [29] has shown promise in text generation. In particular, SEDD has achieved comparable results to auto-regressive models on 5 zero-shot language modeling benchmarks at the GPT-2 scale. Meanwhile, SEDD can reduce the number of function evaluations (NFEs) in sampling and fulfill text conditioned on prompts at different positions.

*Corresponding Author.

Technically, SEDD employs a discrete-state (absorbing) Markov process that adds noises to data by randomly replacing a token with a mask token $[M]$ and then learns a reverse process to denoise from an entirely masked sentence. The key quantities to be estimated in SEDD are the ratios between the marginal probabilities of two transitive states at all timesteps, called the **concrete score**. SEDD also proposes a “scaling trick” (see details in Section 3) that scales the output of the score estimation by a factor. The trick has been proven very effective in practice yet not fully understood in theory [29].

One of our main contributions is to reveal that the concrete score in absorbing diffusion can be expressed as conditional probabilities of clean data, multiplied by a time-dependent scalar in an analytic form (see Theorem 1). Our finding theoretically explains the benefits of the scaling trick as a reparameterization for better optimization. Motivated by the finding, we propose reparameterized absorbing discrete diffusion (RADD), a dedicated diffusion model that characterizes the time-independent conditional probabilities by removing the time conditions from the score estimation. Besides its simplicity, RADD can significantly reduce the NFEs by caching the output of the time-independent network when the noisy sample remains unchanged during a sampling interval (see Fig. 1).

Built upon the new understanding of the concrete score, we further unify absorbing discrete diffusion and any-order autoregressive models (AO-ARMs) [30, 31, 32], demonstrating that their training objectives are equivalent (see Theorem 2). To establish the theory, we first rewrite the original training objective for absorbing discrete diffusion into a simpler form (named t -denoising cross-entropy, t -DCE). Then, we apply a change of variable from the time t to the probability that a single-dimensional token is masked at time t in the forward process. By integrating the probability variable analytically, we show its equivalence to the training objectives for AO-ARMs. These theoretical findings offer a fresh perspective that the upper bound on the negative log-likelihood of an absorbing discrete diffusion can be interpreted as the expected negative log-likelihood for corresponding AO-ARMs. Furthermore, they provide alternative objective functions for training and likelihood evaluation.

Empirically, RADD is up to 3.5 times faster in sampling while consistently achieving similar performance to the strongest baseline, i.e., SEDD [29]. Moreover, we train our RADD models on different objective functions, achieving state-of-the-art performance among diffusion models on five zero-shot language modeling benchmarks (measured by perplexity) at the GPT-2 scale. This empirical evidence validates our theoretical findings.

In summary, this paper has several contributions:

- **Deeper understanding of discrete diffusion:** Both the factorization form of the concrete score and unified training objective for absorbing discrete diffusion and AO-ARMs reveal important yet overlooked theoretical properties of absorbing discrete diffusion, which explain the mysterious scaling trick, provide practice guidance, and may inspire future work.
- **Simpler parameterization:** By removing the time conditions, we reparameterize the model to focus on a time-independent conditional probability, simplifying the existing model.
- **Efficient sampling:** Leveraging the reparameterized form, RADD with a caching strategy achieves consistently faster sampling.
- **Enhanced zero-shot language modeling performance:** Our architectural simplifications and optimized training loss lead to superior results. On five zero-shot language modeling benchmarks, RADD achieves state-of-the-art performance among discrete diffusion models (measured by perplexity) at the GPT-2 scale.

2 Background

In this section, we introduce notations and preliminaries on continuous-time discrete diffusion models in Section 2.1 and any-order autoregressive models in Section 2.2.

Notation We begin by establishing the notations used throughout the paper. Let lower, boldface lower and upper case letters represent scalars (e.g., a), vectors (e.g., \mathbf{a}), and matrices (e.g., \mathbf{A}), respectively. For a vector \mathbf{a} , a^i denotes its i -th element. For a matrix \mathbf{A} , $\mathbf{A}(i, j)$ denotes (i, j) -th element. For a vector function \mathbf{f} , $\mathbf{f}(\mathbf{x})_i$ denotes the i -th element of $\mathbf{f}(\mathbf{x})$. Constants and random variables are not distinguished in the notation if there is no confusion. We represent the distributions of the forward and reverse processes by p and q_θ respectively. The transition probability from time

s to time t is denoted by $p_{t|s}(\cdot|\cdot)$, and the probability at time t is denoted by $p_t(\cdot)$. For complete notations and definitions, see Appendix A.

2.1 Continuous time discrete diffusion model

Single dimension Let x denote a single dimensional sample with possible values in $\mathcal{X} = \{1, \dots, N\}$. A continuous-time discrete Markov chain at time t is characterized by a transition rate matrix \mathbf{Q}_t as follows

$$p_{t+\Delta t|t}(\hat{x}|x) = \begin{cases} \mathbf{Q}_t(x, \hat{x})\Delta t + o(\Delta t), & \hat{x} \neq x, \\ 1 + \mathbf{Q}_t(x, x)\Delta t + o(\Delta t), & \hat{x} = x, \end{cases} \quad (2.1)$$

where $\mathbf{Q}_t(x, \hat{x})$ is the (x, \hat{x}) element of transition rate matrix \mathbf{Q}_t , denoting the transition rate from state x to state \hat{x} at time t . Equivalently, $\mathbf{Q}_t(x, \hat{x})$ is defined as

$$\mathbf{Q}_t(x, \hat{x}) = \begin{cases} \lim_{\Delta t \rightarrow 0} \frac{p_{t+\Delta t|t}(\hat{x}|x) - p_t(x|x)}{\Delta t}, & \hat{x} \neq x, \\ \lim_{\Delta t \rightarrow 0} \frac{p_{t+\Delta t|t}(x|x) - 1}{\Delta t}, & \hat{x} = x. \end{cases} \quad (2.2)$$

Given the above definition, denote $\mathbf{P}_{t|s}(x, \hat{x}) := p_{t|s}(\hat{x}|x)$. The following Kolmogorov's forward equation holds [26, 33]:

$$\frac{d}{dt} \mathbf{P}_{t|s} = \mathbf{P}_{t|s} \mathbf{Q}_t. \quad (2.3)$$

In practice [26, 29], \mathbf{Q}_t is parameterized as $\sigma(t)\mathbf{Q}$, where $\sigma(t)$ is a scalar function representing the noise schedule and \mathbf{Q} is a constant matrix. In this case, the solution to Eq. (2.3) can be solved analytically as $\mathbf{P}_{t|s} = \exp((\bar{\sigma}(t) - \bar{\sigma}(s))\mathbf{Q})$, where $\bar{\sigma}(t) = \int_0^t \sigma(s)ds$ and \exp is the matrix exponential. Therefore, we can directly sample x_t from x_s in one step for any $t > s$.

Further, \mathbf{Q} is often designed to diffuse towards a uniform distribution or an absorbing state [M]. Recent work [20, 26] suggests that the absorbing matrix achieves better empirical performance. Besides, as detailed in Section 3, the specific structure of the absorbing matrix can be leveraged to improve performance and accelerate sampling. Therefore, we focus on the absorbing matrix as follows:

$$\mathbf{Q}^{\text{absorb}} = \begin{bmatrix} -1 & 0 & \dots & 0 & 1 \\ 0 & -1 & \dots & 0 & 1 \\ \vdots & \vdots & \ddots & \vdots & \vdots \\ 0 & 0 & \dots & -1 & 1 \\ 0 & 0 & \dots & 0 & 0 \end{bmatrix}. \quad (2.4)$$

The time reversal of the forward process is characterized by a reverse transition rate matrix $\tilde{\mathbf{Q}}_t$ [34, 35], whose element from state x_t to state \hat{x}_t is given by

$$\tilde{\mathbf{Q}}_t(x_t, \hat{x}_t) = \begin{cases} \frac{p_t(\hat{x}_t)}{p_t(x_t)} \mathbf{Q}_t(\hat{x}_t, x_t), & \hat{x}_t \neq x_t, \\ -\sum_{k \neq x_t} \tilde{\mathbf{Q}}_t(x_t, k), & \hat{x}_t = x_t. \end{cases} \quad (2.5)$$

Simulating the reverse process requires learning the reverse transition rate $\tilde{\mathbf{Q}}_t(x_t, \hat{x}_t)$. As $\mathbf{Q}_t(\hat{x}_t, x_t)$ is known, it is sufficient to estimate the concrete score $\frac{p_t(\hat{x}_t)}{p_t(x_t)}$ by a score network $s_\theta(x_t, t) \approx \left[\frac{p_t(\hat{x}_t)}{p_t(x_t)} \right]_{\hat{x}_t \in \mathcal{X}}$ [28]. Denoising score entropy (DSE) [29] is an effective objective to train the score network

$$\int_0^T \mathbb{E}_{x_t \sim p_{t|0}(x_t|x_0)} \sum_{\hat{x}_t \neq x_t} \mathbf{Q}_t(\hat{x}_t, x_t) \left(s_\theta(x_t, t)_{\hat{x}_t} - \frac{p_{t|0}(\hat{x}_t|x_0)}{p_{t|0}(x_t|x_0)} \log s_\theta(x_t, t)_{\hat{x}_t} + K \left(\frac{p_{t|0}(\hat{x}_t|x_0)}{p_{t|0}(x_t|x_0)} \right) \right) dt, \quad (2.6)$$

where $K(a) := a \log a - a$. In particular, the DSE loss in Eq. (2.6) is an upper bound of the negative log-likelihood with an unknown gap. Nevertheless, existing work [29] still employs it for training and likelihood evaluation.

After training, sampling can be understood as discretizing the following reverse process

$$\frac{d}{ds} P_{s|t} = P_{s|t} \tilde{Q}_s, \quad (2.7)$$

where ds is an infinitesimal negative timestep and the concrete score is replaced by the score network. Existing samplers include the Euler method and Tweedie τ -leaping, as detailed in Appendix D.

Multi-dimension In a state space of length d like $\mathcal{X}^d = \{1, \dots, n\}^d$, we denote the sample as a sequence of one-dimensional data, i.e., $\mathbf{x} = x^1 \dots x^d$. The transition matrix $\mathbf{Q}_t \in \mathbb{R}^{n^d \times n^d}$ has an exponential number of possible states, making it expensive to reverse. To alleviate this issue, existing work [26, 29] assumes independence between dimensions and each dimension is a one-dimensional diffusion process with the same transition rate matrix $\mathbf{Q}_t^{\text{tok}} \in \mathbb{R}^{n \times n}$.

Under the independent assumption, \mathbf{Q}_t assigns zero values [26, 29] for all sequences with a Hamming distance larger than 1. Therefore, it is sufficient to model the concrete score between sequences that differ by a Hamming distance of 1, such as $\hat{\mathbf{x}}_t = x_t^1 \dots \hat{x}_t^i \dots x_t^d$ given $\mathbf{x}_t = x_t^1 \dots x_t^d$. Therefore, the score network $\mathbf{s}_\theta(\cdot, t) : \{1, \dots, n\}^d \rightarrow \mathbb{R}^{d \times n}$ is defined as

$$\mathbf{s}_\theta(\mathbf{x}_t, t)_{\hat{\mathbf{x}}_t} = \mathbf{s}_\theta(x_t^1 \dots x_t^i \dots x_t^d, t) [i, \hat{x}_t^i] \approx \frac{p_t(x_t^1 \dots \hat{x}_t^i \dots x_t^d)}{p_t(x_t^1 \dots x_t^i \dots x_t^d)}, \quad (2.8)$$

which leads to the following expression to estimate the reverse transition rate matrix \tilde{Q}_t :

$$\tilde{Q}_t(x_t^1 \dots x_t^i \dots x_t^d, x_t^1 \dots \hat{x}_t^i \dots x_t^d) = \mathbf{Q}_t^{\text{tok}}(\hat{x}_t^i, x_t^i) \frac{p_t(x_t^1 \dots \hat{x}_t^i \dots x_t^d)}{p_t(x_t^1 \dots x_t^i \dots x_t^d)} \quad (2.9)$$

$$\approx \mathbf{Q}_t^{\text{tok}}(\hat{x}_t^i, x_t^i) \mathbf{s}_\theta(x_t^1 \dots x_t^i \dots x_t^d, t) [i, \hat{x}_t^i]. \quad (2.10)$$

Existing samplers assume that each dimension is independent within a small interval Δt and update each dimension in parallel for efficiency [29, 26].

2.2 Any-order autoregressive models

Any-order autoregressive models (AO-ARMs) [30, 31, 32] model the joint distribution autoregressively for all possible orders π of the d variables. Formally, they factorize the joint distribution as $\prod_{k=1}^d p(x^{\pi(k)} | x^{\pi(<k)})$. To learn such a distribution, an AO-ARM utilizes a weight-sharing neural network to model all univariate conditionals and employs mask tokens to represent absent variables. During training, the expected negative log-likelihood over the uniform distribution of all orders U_π is minimized:

$$\mathcal{L}_{AO}(\mathbf{x}_0) = \mathbb{E}_{\pi \sim U_\pi} \sum_{l=1}^d \log q_\theta(x_0^{\pi(l)} | x_0^{\pi(<l)}; \pi). \quad (2.11)$$

3 Reparameterized absorbing discrete diffusion

In Section 3.1, we reveal that the concrete score of absorbing discrete diffusion can be reparameterized as conditional distributions of clean data, which enables efficient sampling by caching the output of time-independent network (see Section 3.2). In Section 3.3, we unify the training objective of absorbing discrete diffusion and AO-ARMs.

3.1 Parameterizing the concrete score as conditional distributions of clean data

A key observation is that only the transition from the masked token to an unmasked token is valid in the reverse process of an absorbing discrete diffusion. In particular, according to the definition of the transition matrix of the absorbing process (see Eq. (2.4)), we have $\mathbf{Q}^{\text{absorb}}(\hat{x}_t^i, x_t^i) = 0$ for any unmasked $x_t^i \neq [\mathbf{M}]$ and $\hat{x}_t^i \neq x_t^i$. Therefore, the corresponding element in the transition matrix of the reverse process \tilde{Q}_t (see Eq. (2.5)) equals zero. Namely,

$$\tilde{Q}_t(x_t^1 \dots x_t^i \dots x_t^d, x_t^1 \dots \hat{x}_t^i \dots x_t^d) = \sigma(t) \mathbf{Q}^{\text{absorb}}(\hat{x}_t^i, x_t^i) \frac{p_t(x_t^1 \dots \hat{x}_t^i \dots x_t^d)}{p_t(x_t^1 \dots x_t^i \dots x_t^d)} = 0, \quad (3.1)$$

for any unmasked state $x_t^i \neq [\mathbf{M}]$ and $\hat{x}_t^i \neq x_t^i$ and it is unnecessary to model the corresponding concrete score $\frac{p_t(x_t^1 \dots \hat{x}_t^i \dots x_t^d)}{p_t(x_t^1 \dots x_t^i \dots x_t^d)}$. Also, note that the concrete score always takes the value of one if $\hat{x}_t^i = x_t^i$. Therefore, we only need to characterize the concrete score for $x_t^i = [\mathbf{M}]$ and $\hat{x}_t^i \neq [\mathbf{M}]$.

Interestingly, in this case, we discover that the concrete score has a simple analytic form w.r.t. to the conditional distributions of clean data, as summarized in the following Theorem 1.

Theorem 1. (Analytic concrete score in absorbing diffusion, proof in Appendix B) For $\mathbf{x}_t = x_t^1 \dots x_t^i \dots x_t^d$ and $\hat{\mathbf{x}}_t = x_t^1 \dots \hat{x}_t^i \dots x_t^d$, if $x_t^i = [\mathbf{M}]$ and $\hat{x}_t^i \neq [\mathbf{M}]$, the concrete score at time t can be expressed as a *time-independent* conditional distribution at time zero multiplied by an analytic *time-dependent* term:

$$\frac{p_t(x_t^1 \dots \hat{x}_t^i \dots x_t^d)}{p_t(x_t^1 \dots x_t^i \dots x_t^d)} = \frac{e^{-\bar{\sigma}(t)}}{1 - e^{-\bar{\sigma}(t)}} p_0(\hat{x}_t^i | \mathbf{x}_t^{UM}),$$

where \mathbf{x}_t^{UM} is the vector consists of all unmasked tokens of \mathbf{x}_t .

One immediate implication of Theorem 1 is to theoretically explain the benefit of the ‘‘scaling trick’’ in existing work [29] (see Appendix C.2 therein), which significantly improves the practical performance of discrete diffusion (see Table 1) but has not been fully understood before. In particular, the scaling trick divides the output of the score network by a factor. Equivalently, it reparameterizes $s_\theta(\mathbf{x}_t, t)$ as follows:

$$s_\theta(\mathbf{x}_t, t) = \frac{e^{-\bar{\sigma}(t)}}{1 - e^{-\bar{\sigma}(t)}} \bar{s}_\theta(\mathbf{x}_t, t),$$

where $\bar{s}_\theta(\mathbf{x}_t, t)$ is the output of the reparameterized score network and the scaling factor coincides with the time-dependent term in Theorem 1. In the original parameterization, the score network s_θ must model the whole time-dependent concrete score. In contrast, with the scaling trick, the reparameterized score $\bar{s}_\theta(\mathbf{x}_t, t)$ can focus on capturing the clean data distribution $p_0(\hat{x}_t^i | \mathbf{x}_t^{UM})$ and simplifies learning, according to Theorem 1.

Further, Theorem 1 suggests that the reparameterized score is essentially a conditional probability on clean data, which is time-independent. Motivated by the insights, we propose reparameterized absorbing discrete diffusion (RADD), which employs a time-independent network $c_\theta(\mathbf{x}_t)$ that defines a model distribution q_θ by corresponding conditional distributions to approximate data distribution p_0 directly:

$$c_\theta(\mathbf{x}_t)[i, \hat{x}_t^i] = q_\theta(\hat{x}_t^i | \mathbf{x}_t^{UM}) \approx p_0(\hat{x}_t^i | \mathbf{x}_t^{UM}). \quad (3.2)$$

In practice, we make a minimal modification of the score network in SEDD [29] for simplicity and fairness. Briefly, we remove the time condition from the input and take the softmax as the final nonlinearity. Further details can be found in Appendix G.1.

Moreover, RADD also enjoys a more efficient sampling process than SEDD [29] based on its simplified parameterization, as presented below.

3.2 Efficient samplers to reduce NFEs by caching the output of RADD

In the reverse process of an absorbing discrete diffusion, once a token transitions from $[\mathbf{M}]$ to an unmasked token, it remains unchanged. Consequently, for a sequence consisting of d tokens, there will be at most d intervals during the sampling process where changes occur, regardless of the number of sampling steps D . In the remaining steps, the sequence remains unchanged across all d dimensions. This property allows us to cache $c_\theta(\mathbf{x}_t)$ to avoid the need to reevaluate the time-independent c_θ when \mathbf{x}_t is unchanged in the previous step (see Appendix F for the pseudo-code). However, since SEDD is conditioned on time, it does not support this caching strategy for reducing NFEs.

The NFEs with the caching strategy is a random variable. To quantify it, we calculate the expected NFEs (E-NFEs) in analytic form, conditioned on the sampling method, time steps, and noise schedule. For instance, using the Tweedie τ -leaping method with a log-linear noise schedule [29], the E-NFEs

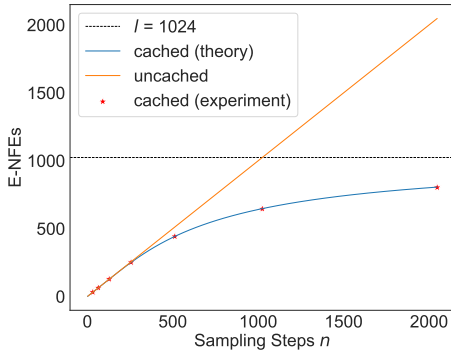


Figure 1: **Expected number of function evaluations (E-NFEs) over a different number of sampling steps.** E-NFEs is measured by Tweedie τ -leaping method with log-linear noise schedule.

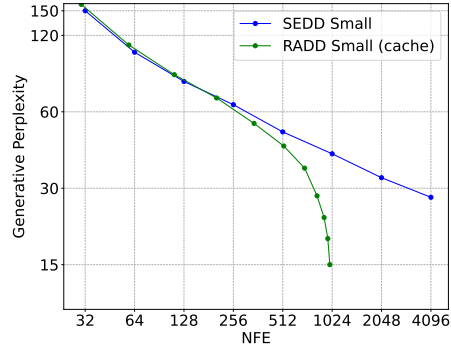


Figure 2: **Sample quality measured by perplexity (\downarrow).** The x-axis represents E-NFEs for RADD with caching strategy and NFEs for SEDD. RADD with cache strategy achieves $2 \sim 3.5\times$ speedup compared to SEDD with steps ranging from 1024 to 4096.

is given by (proof in Appendix D.5):

$$\text{E-NFEs}(n) = n\left(1 - \left(1 - \frac{1}{n}\right)^l\right), \quad (3.3)$$

where n represents the sampling steps and l represents the length to be generated.

In Fig. 1, we plot the curve of Eq. (3.3) in blue, which aligns well with our experiments (the red stars). This demonstrates that our method theoretically reduces E-NFEs significantly when the number of sampling steps is large, and this reduction is also confirmed experimentally in Fig. 2.

Furthermore, based on Theorem 1, simplified forms of the reverse process for both Euler method and Tweedie τ -leaping method can be derived, which leads to corresponding analytic forms of E-NFEs given time steps and noise schedule. We also prove that these two sampling methods are equivalent under a log-linear noise schedule for absorbing discrete diffusion (see Appendix D for more details).

3.3 Unifying absorbing discrete diffusion and any-order autoregressive models

Building upon Theorem 1, we further prove the equivalence between absorbing discrete diffusion and any-order autoregressive models [30, 31, 32], as presented in the following theorem.

Theorem 2. *The absorbing discrete diffusion objective of Eq. (2.6) is equivalent to any-order autoregressive objective of Eq. (2.11) when the final total noise level $\bar{\sigma}(T) \rightarrow +\infty$.*

The proof of Theorem 2 consists of three key steps, which introduce three different yet equivalent loss functions. Below we briefly present the key ideas and defer the proof in Appendix C.

In the first step, by removing the terms $s_\theta(\mathbf{x}_t, t)_{\hat{\mathbf{x}}_t}$ and $K\left(\frac{p_{t|0}(\hat{\mathbf{x}}_t|\mathbf{x}_0)}{p_{t|0}(\mathbf{x}_t|\mathbf{x}_0)}\right)$ in Eq. (2.6), we can define a simpler loss $\mathcal{L}_{t\text{-DCE}}^T$ called t -denoising cross-entropy loss (abbr. t -DCE), which is equivalent to DSE loss. In the multi-dimensional case, it has the form:

$$\mathcal{L}_{t\text{-DCE}}^T(\mathbf{x}_0) = \int_0^T \mathbb{E}_{\mathbf{x}_t \sim p_{t|0}(\mathbf{x}_t|\mathbf{x}_0)} \left[\sum_{x_t^i = [\mathbf{M}]} -\frac{\sigma(t)e^{-\bar{\sigma}(t)}}{1 - e^{-\bar{\sigma}(t)}} \log \left(\frac{e^{-\bar{\sigma}(t)}}{1 - e^{-\bar{\sigma}(t)}} q_\theta(x_0^i | \mathbf{x}_t^{\text{UM}}) \right) \right] dt. \quad (3.4)$$

We emphasize that Eq. (3.4) holds in a nonparametric setting because RADD can be interpreted as a model distribution q_θ representing the conditional distribution of clean data, which approximates the true distribution p_0 , as proven in Theorem 1.

In the second step, inspired by Kingma et al. [36], we change the variable from t to $\lambda(t) = 1 - e^{-\bar{\sigma}(t)}$, which represents the probability of a token being masked in $[0, t]$ during the forward process. Thus, $\mathcal{L}_{t\text{-DCE}}^T(\mathbf{x}_0)$ can be rewritten as an integral of λ , defined as λ -denoising cross-entropy loss (abbr. λ -DCE):

$$\mathcal{L}_{\lambda\text{-DCE}}(\mathbf{x}_0) := \int_0^1 \frac{1}{\lambda} \mathbb{E}_{\mathbf{x}_\lambda \sim p_\lambda(\mathbf{x}_\lambda | \mathbf{x}_0)} \left[\sum_{x_\lambda^i = [\mathbf{M}]} -\log q_\theta(\mathbf{x}_0^i | \mathbf{x}_\lambda^{\text{UM}}) \right] d\lambda, \quad (3.5)$$

where $p_\lambda(\mathbf{x}_\lambda | \mathbf{x}_0)$ is the joint distribution induced by masking each dimension in \mathbf{x}_0 independently with a probability λ .

Finally, we prove that λ -DCE loss in Eq. (3.5) can be integrated analytically and rewritten as \mathcal{L}_{AO} in Eq. (2.11). We summarize our proof procedure by the equivalence between these losses:

$$\mathcal{L}_{\text{DSE}}^T(\mathbf{x}_0) \stackrel{\text{Appendix C.1}}{\iff} \mathcal{L}_{t\text{-DCE}}^T(\mathbf{x}_0) \stackrel{\text{Appendix C.2}}{\iff} \mathcal{L}_{\lambda\text{-DCE}}(\mathbf{x}_0) \stackrel{\text{Appendix C.3}}{\iff} \mathcal{L}_{AO}(\mathbf{x}_0). \quad (3.6)$$

A direct benefit from Theorem 2 is that we can use an absorbing discrete diffusion model to sample like AO-ARM and vice versa. For training and likelihood evaluation, the four losses in Eq. (3.6) can also be used (see Appendix F for pseudo-code). To efficiently estimate the four losses using Monte Carlo methods, we can replace the sum or integral with an expectation. Take Eq. (3.5) for example, it can be rewritten as the following form of expectation on λ :

$$\mathcal{L}_{\lambda\text{-DCE}}(\mathbf{x}_0) = \mathbb{E}_{\lambda \sim U([0,1])} \frac{1}{\lambda} \mathbb{E}_{\mathbf{x}_\lambda \sim p_\lambda(\mathbf{x}_\lambda | \mathbf{x}_0)} \left[\sum_{x_\lambda^i = [\mathbf{M}]} -\log q_\theta(\mathbf{x}_0^i | \mathbf{x}_\lambda^{\text{UM}}) \right]. \quad (3.7)$$

Additionally, Theorem 2 provides a new perspective on the DSE loss. While it has been traditionally viewed as an upper bound on the negative log-likelihood for the diffusion model, it can also be interpreted as an expected negative log-likelihood over factorial numbers of orderings for AO-ARM by Eq. (2.11). As discussed in [30], for different orders π , $q_\theta(x_0; \pi)$ will be inconsistent in general. Despite this inconsistency, it can be viewed as an ensemble of multiple autoregressive models with different orders, potentially more robust than fixed-order models.

4 Experiments

We present the experimental setups in Section 4.1. We then evaluate the performance of accelerated generation in Section 4.2 and zero-shot perplexity on various language datasets in Section 4.3.

4.1 Settings

Below, we briefly present the experimental settings. For more details, please see Appendix G.

Model. We use RADD model c_θ reparameterized as described in Section 3.1. Compared with SEDD small model, RADD model has 7M fewer parameters due to the removal of time-condition, which equates to an 8% decrease from the original 90M non-embedding parameters. We trained our RADD model c_θ using denoising score entropy, t -denoising cross-entropy, λ -denoising cross-entropy and any-order autoregressive loss, abbreviated as RADD-DSE, RADD- t -DCE, RADD- λ -DCE and RADD-AO. For the SEDD small model, we employed their pre-trained model. In text generation tasks, we used RADD- t -DCE.

Data. Following SEDD, we trained on the OpenWebText [37] dataset and tested on the LAMBADA, WikiText2, PTB, WikiText103, and One Billion Words datasets [38, 39, 40, 41]. For data splits and data processing, we adopted the same settings and techniques as SEDD, which involves packing sentences to generate uniform-length blocks as model input.

Training setup. We used a log-linear noise schedule where the expectation of the number of changed tokens at time t is linear with t . For RADD-DSE, we use the same hyperparameter with SEDD for fair comparison. For other RADD models, we referenced the hyperparameter in [42].

Metric. Following previous work [29], we conduct experiments on unconditional generation and language modeling tasks. For generation, we use perplexity (PPL) on unconditional samples measured by an additional larger language model (i.e., GPT-2 large) to evaluate sample quality. For language modeling tasks, we report the perplexity calculated on the dataset with different models.

4.2 Efficient sampling

We compare the sample quality measured by perplexity between SEDD and our RADD- t -DCE model under a log-linear noise schedule. As shown in Fig. 2, RADD with the caching strategy is more efficient than SEDD, with efficiency gains increasing as the number of sample steps increases. This improvement is expected because the NFEs is limited by the generating sequence length. We further compare the running time as detailed in Appendix G.4.

As discussed in Section 3.3, we can also use RADD as an any-order autoregressive model to generate samples in different orders, leading to worse performance as a discrete diffusion, as detailed in Appendix G.4. We present more sampling details in Appendix G.3. and the generated samples in Appendix H.1.

4.3 Improved zero-shot perplexity on language modeling

Following SEDD, we present zero-shot perplexities on the LAMBADA, WikiText2, PTB, WikiText103, and 1 Billion Words datasets [43] in Table 1² and compare the zero-shot perplexity of our model with other baseline models [20, 44, 29]. This table reports results for RADD models trained for 400k iterations. Further, we provide the results of RADD models that are trained with 1000k iterations in Table 2.

Firstly, we conduct an ablation study of the scaling trick in the middle of the Table 1. For the absorbing diffusion, the perplexity of the scaled version of SEDD outperforms its unscaled version, which matches our theoretical discovery in Theorem 1.

Secondly, with the same DSE loss and hyperparameters, we observed that the RADD-DSE model without time-conditioning performs comparably to the SEDD-S model with time-conditioning. This validates our analysis in Section 3.1, indicating that time-conditioning is unnecessary for absorbing discrete diffusion models.

Thirdly, we report the results of RADD models trained on other equivalent losses in the last three rows of the Table 1 and Table 2. Their perplexities are calculated based on their corresponding loss (e.g., RADD- λ -DCE on $\mathcal{L}_{\lambda\text{-DCE}}$), which is valid for likelihood estimation as discussed in Section 3.3. We observed that the RADD- t -DCE and RADD-AO consistently outperform SEDD, while RADD- λ -DCE also outperforms SEDD on all tasks except LAMBADA. These results demonstrate the correctness of our conclusion in Section 3.3 while showing that the empirical contributions of [42] also apply to RADD for better performance.

5 Related work

Continuous-state diffusion models for text generation. Several works have been proposed to apply continuous diffusion to text [19, 21, 22, 23]. Li et al. [19] use an embedding layer to map discrete tokens to a latent space and learn a continuous-state diffusion on it. Bit Diffusion [22] learns a continuous diffusion model to generate binary bits of discrete tokens. However, transforming between these continuous representations and discrete tokens by thresholding may lose information. Bayesian Flow Network [23] achieves competitive log-likelihood on character-level language modeling tasks and is proven equivalent to continuous stochastic differential equations trained by denoising score matching [24]. Such models underperform auto-regressive models on standard text generation tasks.

Discrete-state diffusion models for text generation. Several discrete-state diffusion models have been proposed [11, 45, 20]. D3PM [20] proposed a diffusion framework based on any probability transition matrix and trained with a lower bound of log-likelihood. DiffusionBERT [25] utilizes a

²In the initial version of the RADD model, we mistakenly removed the time-dependent bias term in the layernorm layer without adding a bias term that is independent of time. In the latest implementation, we have fixed this bug.

Table 1: **Zero-shot language modeling perplexity (\downarrow) on five datasets.** SEDD-U / SEDD-S refer to the unscaled and scaled absorbing models, respectively. All SEDD and RADD models are trained for **400k** iterations. Results for general diffusion models are based on the upper bound which is taken from [20, 44, 29]. For RADD models, the results are calculated based on corresponding loss.

Method	LAMBADA	WikiText2	PTB	WikiText103	1BW
GPT-2	45.04	42.43	138.43	41.60	75.20
D3PM	93.47	77.28	200.82	75.16	138.92
PLAID	57.28	51.80	142.60	50.86	91.12
SEDD-Uniform	65.40	50.27	140.12	49.60	101.37
SEDD-U	52.21	44.75	130.49	43.14	80.70
SEDD-S	50.92	41.84	114.24	40.62	79.29
RADD-DSE	51.83	40.34	116.57	37.80	76.27
RADD- t -DCE	50.56	39.02	109.03	36.38	72.60
RADD- λ -DCE	51.70	39.98	107.85	37.98	72.99
RADD-AO	50.27	38.26	110.38	35.90	74.28

Table 2: **Additional zero-shot language modeling perplexity (\downarrow) for RADD models.** We present the perplexity for RADD models trained for **1000k** iterations based on their corresponding loss.

Method	LAMBADA	WikiText2	PTB	WikiText103	1BW
RADD- t -DCE	48.92	37.44	102.49	37.20	70.58
RADD- λ -DCE	49.74	37.13	98.84	36.66	69.77
RADD-AO	49.43	36.86	102.36	35.25	70.71

pre-trained BERT [46] as an initialization of diffusion. Furthermore, [26] generalizes the framework to continuous time by introducing a rate matrix. It is difficult to apply the score matching in such models because the gradient of the data distribution is undefined. Several works try to generalize the score matching on discrete data [29, 28, 26, 27]. Meng et al. [28] introduce the concrete score and the denoising concrete score matching loss. Furthermore, SEDD bridges the discrete state diffusion and the concrete score by introducing a denoising score entropy loss [29]. By incorporating an absorbing process, SEDD achieves competitive performance with the auto-regressive models, especially, GPT-2.

Concurrent works We mention that Shi et al. [42] and Sahoo et al. [47] independently conducted related studies on absorbing discrete diffusion and we provide a comprehensive discussion here.

Shi et al. [42] derived a weighted integral of cross-entropy loss in their Eq.(5) similar to our t -DCE loss in Eq. (3.4). Besides, their Proposition 1, which connects the score parameterization and the mean parameterization³, also resembles our Theorem 1. In comparison, we simplified the conditional expectation term (related to t) in Proposition 1 [42] to a time-independent conditional probability at time zero. Motivated by the finding, we proposed a simpler parameterization that enables fast sampling. It is worth noting that the hyperparameters they selected significantly contribute to the model’s performance, which also applies to our RADD models (see Appendix G.2 for details). In addition, Shi et al. [42] proposed a generalized masked diffusion model allowing state-dependent masking schedules.

Sahoo et al. [47] derive the same cross-entropy losses with Shi et al. [42]. Despite lacking a theoretical foundation, they conducted time-conditioning ablation which shows that time-conditioning has minimal impact on perplexity. They also proposed a caching strategy to accelerate sampling. While this coincides with our work in Section 3.2, we present a complete theoretical analysis of E-NFEs to quantify the acceleration efficiency.

³Our conclusions are based on score parameterization but can be extended to mean prediction parameterization (please see Appendix E).

Compared with the concurrent works, our research offers a complementary perspective on absorbing diffusion, reveals its time-independent property, proposes a theoretically sound cache strategy for fast sampling, derives two additional loss functions, and connects it to any-order autoregressive models.

6 Conclusion

We introduce RADD, a dedicated discrete diffusion model that characterizes the time-independent conditional probabilities, built upon a new factorization form of the concrete score. RADD is much more efficient by reducing the NFEs with a cache strategy while maintaining comparable performance to strong baselines. Additionally, we demonstrated the unification of training objectives for absorbing discrete diffusion and AO-ARMs. On five zero-shot language modeling benchmarks, our RADD models achieve state-of-the-art performance at the GPT-2 scale.

Limitation. Our model has been trained and evaluated primarily on the GPT-2 scale. For broader applicability, it is essential to explore the effects of scaling on the performance [48], which is left as future work. The success of diffusion transformers on images [49, 50, 51] and videos [52] suggests that diffusion models can be scaled up by incorporating transformers.

Another limitation is that our model can only generate full-length outputs, unlike auto-regressive models that can produce variable-length outputs. This restricts the flexibility of our model in certain applications. We leave the investigation on this issue as future work.

Social impact. For the current theoretical and experimental scope of this paper, we have not found any direct social impacts. However, considering future developments, the paper potentially contributes to the next-generation large language models. In this context, this work could significantly reduce the inference cost of language models but may also lead to hallucinations, amplify biases and discrimination in the data, and pose risks of misuse. As with other generative models, addressing these issues requires further advancements in the field.

Acknowledgments

We thank Aaron Lou for his prompt and detailed responses to our inquiries, which greatly assisted our research. We also thank Zebin You for his support in setting up the coding environment.

References

- [1] Alec Radford, Karthik Narasimhan, Tim Salimans, Ilya Sutskever, et al. Improving language understanding by generative pre-training. *OpenAI blog*, 2018.
- [2] Alec Radford, Jeffrey Wu, Rewon Child, David Luan, Dario Amodei, Ilya Sutskever, et al. Language models are unsupervised multitask learners. *OpenAI blog*, 1(8):9, 2019.
- [3] Tom Brown, Benjamin Mann, Nick Ryder, Melanie Subbiah, Jared D Kaplan, Prafulla Dhariwal, Arvind Neelakantan, Pranav Shyam, Girish Sastry, Amanda Askell, et al. Language models are few-shot learners. *Advances in neural information processing systems*, 33:1877–1901, 2020.
- [4] Ashish Vaswani, Noam Shazeer, Niki Parmar, Jakob Uszkoreit, Llion Jones, Aidan N Gomez, Łukasz Kaiser, and Illia Polosukhin. Attention is all you need. *Advances in neural information processing systems*, 30, 2017.
- [5] OpenAI. ChatGPT: Optimizing Language Models for Dialogue. *OpenAI blog*, November 2022. URL <https://openai.com/blog/chatgpt/>.
- [6] Josh Achiam, Steven Adler, Sandhini Agarwal, Lama Ahmad, Ilge Akkaya, Florencia Leoni Aleman, Diogo Almeida, Janko Altenschmidt, Sam Altman, Shyamal Anadkat, et al. Gpt-4 technical report. *arXiv preprint arXiv:2303.08774*, 2023.
- [7] Hugo Touvron, Thibaut Lavril, Gautier Izacard, Xavier Martinet, Marie-Anne Lachaux, Timothée Lacroix, Baptiste Rozière, Naman Goyal, Eric Hambro, Faisal Azhar, Aurelien Rodriguez, Armand Joulin, Edouard Grave, and Guillaume Lample. Llama: Open and efficient foundation language models, 2023.

- [8] Rohan Anil, Andrew M Dai, Orhan Firat, Melvin Johnson, Dmitry Lepikhin, Alexandre Passos, Siamak Shakeri, Emanuel Taropa, Paige Bailey, Zhifeng Chen, et al. Palm 2 technical report. *arXiv preprint arXiv:2305.10403*, 2023.
- [9] Lukas Berglund, Meg Tong, Max Kaufmann, Mikita Balesni, Asa Cooper Stickland, Tomasz Korbak, and Owain Evans. The reversal curse: LLMs trained on "a is b" fail to learn "b is a". *arXiv preprint arXiv:2309.12288*, 2023.
- [10] Ang Lv, Kaiyi Zhang, Shufang Xie, Quan Tu, Yuhan Chen, Ji-Rong Wen, and Rui Yan. Are we falling in a middle-intelligence trap? an analysis and mitigation of the reversal curse. *arXiv preprint arXiv:2311.07468*, 2023.
- [11] Jascha Sohl-Dickstein, Eric Weiss, Niru Maheswaranathan, and Surya Ganguli. Deep unsupervised learning using nonequilibrium thermodynamics. In *International conference on machine learning*, pages 2256–2265. PMLR, 2015.
- [12] Jonathan Ho, Ajay Jain, and Pieter Abbeel. Denoising diffusion probabilistic models. *Advances in neural information processing systems*, 33:6840–6851, 2020.
- [13] Yang Song, Jascha Sohl-Dickstein, Diederik P Kingma, Abhishek Kumar, Stefano Ermon, and Ben Poole. Score-based generative modeling through stochastic differential equations. In *International Conference on Learning Representations*, 2021.
- [14] Jiaming Song, Chenlin Meng, and Stefano Ermon. Denoising diffusion implicit models. In *International Conference on Learning Representations*, 2021.
- [15] Fan Bao, Chongxuan Li, Jun Zhu, and Bo Zhang. Analytic-DPM: An analytic estimate of the optimal reverse variance in diffusion probabilistic models. In *International Conference on Learning Representations*, 2022.
- [16] Qinsheng Zhang and Yongxin Chen. Fast sampling of diffusion models with exponential integrator. In *International Conference on Learning Representations*, 2023.
- [17] Cheng Lu, Yuhao Zhou, Fan Bao, Jianfei Chen, Chongxuan Li, and Jun Zhu. Dpm-solver: A fast ode solver for diffusion probabilistic model sampling in around 10 steps. *Advances in Neural Information Processing Systems*, 35:5775–5787, 2022.
- [18] Cheng Lu, Yuhao Zhou, Fan Bao, Jianfei Chen, Chongxuan Li, and Jun Zhu. Dpm-solver++: Fast solver for guided sampling of diffusion probabilistic models. *arXiv preprint arXiv:2211.01095*, 2022.
- [19] Xiang Lisa Li, John Thickstun, Ishaan Gulrajani, Percy Liang, and Tatsunori B. Hashimoto. Diffusion-lm improves controllable text generation, 2022.
- [20] Jacob Austin, Daniel D. Johnson, Jonathan Ho, Daniel Tarlow, and Rianne van den Berg. Structured denoising diffusion models in discrete state-spaces. In *Advances in Neural Information Processing Systems*, 2021.
- [21] Sander Dieleman, Laurent Sartran, Arman Roshannai, Nikolay Savinov, Yaroslav Ganin, Pierre H. Richemond, Arnaud Doucet, Robin Strudel, Chris Dyer, Conor Durkan, Curtis Hawthorne, Rémi Leblond, Will Grathwohl, and Jonas Adler. Continuous diffusion for categorical data, 2022.
- [22] Ting Chen, Ruixiang Zhang, and Geoffrey Hinton. Analog bits: Generating discrete data using diffusion models with self-conditioning, 2023.
- [23] Alex Graves, Rupesh Kumar Srivastava, Timothy Atkinson, and Faustino Gomez. Bayesian flow networks, 2024.
- [24] Kaiwen Xue, Yuhao Zhou, Shen Nie, Xu Min, Xiaolu Zhang, Jun Zhou, and Chongxuan Li. Unifying bayesian flow networks and diffusion models through stochastic differential equations, 2024.

- [25] Zhengfu He, Tianxiang Sun, Kuanning Wang, Xuanjing Huang, and Xipeng Qiu. Diffusionbert: Improving generative masked language models with diffusion models. *arXiv preprint arXiv:2211.15029*, 2022.
- [26] Andrew Campbell, Joe Benton, Valentin De Bortoli, Tom Rainforth, George Deligiannidis, and A. Doucet. A continuous time framework for discrete denoising models. In *Advances in Neural Information Processing Systems*, 2022.
- [27] Haoran Sun, Lijun Yu, Bo Dai, Dale Schuurmans, and Hanjun Dai. Score-based continuous-time discrete diffusion models, 2023.
- [28] Chenlin Meng, Kristy Choi, Jiaming Song, and Stefano Ermon. Concrete score matching: Generalized score matching for discrete data, 2023.
- [29] Aaron Lou, Chenlin Meng, and Stefano Ermon. Discrete diffusion modeling by estimating the ratios of the data distribution, 2024.
- [30] Benigno Uribe, Iain Murray, and Hugo Larochelle. A deep and tractable density estimator. In *Proceedings of the 31th International Conference on Machine Learning*, 2014.
- [31] Emiel Hoogeboom, Alexey A. Gritsenko, Jasmijn Bastings, Ben Poole, Rianne van den Berg, and Tim Salimans. Autoregressive diffusion models. In *10th International Conference on Learning Representations*, 2022.
- [32] Andy Shih, Dorsa Sadigh, and Stefano Ermon. Training and inference on any-order autoregressive models the right way. In *Proceedings of the 31th International Conference on Machine Learning*, 2022.
- [33] William J Anderson. *Continuous-time Markov chains: An applications-oriented approach*. Springer Science & Business Media, 2012.
- [34] Haoran Sun, Lijun Yu, Bo Dai, Dale Schuurmans, and Hanjun Dai. Score-based continuous-time discrete diffusion models. In *The Eleventh International Conference on Learning Representations*, 2023.
- [35] Frank Kelly. Reversibility and stochastic networks / f.p. kelly. *SERBIULA (sistema Librum 2.0)*, 76, 06 1981. doi: 10.2307/2287860.
- [36] Diederik Kingma, Tim Salimans, Ben Poole, and Jonathan Ho. Variational diffusion models. In M. Ranzato, A. Beygelzimer, Y. Dauphin, P.S. Liang, and J. Wortman Vaughan, editors, *Advances in Neural Information Processing Systems*, volume 34, pages 21696–21707. Curran Associates, Inc., 2021.
- [37] Aaron Gokaslan and Vanya Cohen. Openwebtext corpus. <http://Skylion007.github.io/OpenWebTextCorpus>, 2019.
- [38] Denis Paperno, Germán Kruszewski, Angeliki Lazaridou, Ngoc Quan Pham, Raffaella Bernardi, Sandro Pezzelle, Marco Baroni, Gemma Boleda, and Raquel Fernandez. The LAMBADA dataset: Word prediction requiring a broad discourse context. In *Proceedings of the 54th Annual Meeting of the Association for Computational Linguistics (Volume 1: Long Papers)*, pages 1525–1534, Berlin, Germany, August 2016. Association for Computational Linguistics. URL <http://www.aclweb.org/anthology/P16-1144>.
- [39] Stephen Merity, Caiming Xiong, James Bradbury, and Richard Socher. Pointer sentinel mixture models. In *International Conference on Learning Representations*, 2016.
- [40] Mitchell P. Marcus, Beatrice Santorini, and Mary Ann Marcinkiewicz. Building a large annotated corpus of english: The penn treebank. *Comput. Linguistics*, 19:313–330, 1993.
- [41] Ciprian Chelba, Tomas Mikolov, Mike Schuster, Qi Ge, T. Brants, Phillip Todd Koehn, and Tony Robinson. One billion word benchmark for measuring progress in statistical language modeling. In *Interspeech*, 2013.
- [42] Jiaxin Shi, Kehang Han, Zhe Wang, Arnaud Doucet, and Michalis K. Titsias. Simplified and generalized masked diffusion for discrete data, 2024.

- [43] Alec Radford, Jeffrey Wu, Rewon Child, David Luan, Dario Amodei, Ilya Sutskever, et al. Language models are unsupervised multitask learners. *OpenAI blog*, 1(8):9, 2019.
- [44] Ishaan Gulrajani and Tatsunori Hashimoto. Likelihood-based diffusion language models. In *Advances in Neural Information Processing Systems*, 2023.
- [45] Emiel Hoogeboom, Didrik Nielsen, Priyank Jaini, Patrick Forré, and Max Welling. Argmax flows and multinomial diffusion: Learning categorical distributions. *Advances in Neural Information Processing Systems*, 34:12454–12465, 2021.
- [46] Jacob Devlin, Ming-Wei Chang, Kenton Lee, and Kristina Toutanova. BERT: Pre-training of deep bidirectional transformers for language understanding. In *Proceedings of the 2019 Conference of the North American Chapter of the Association for Computational Linguistics: Human Language Technologies, Volume 1 (Long and Short Papers)*. Association for Computational Linguistics, 2019.
- [47] Subham Sekhar Sahoo, Marianne Arriola, Yair Schiff, Aaron Gokaslan, Edgar Marroquin, Justin T Chiu, Alexander Rush, and Volodymyr Kuleshov. Simple and effective masked diffusion language models, 2024.
- [48] Jordan Hoffmann, Sebastian Borgeaud, Arthur Mensch, Elena Buchatskaya, Trevor Cai, Eliza Rutherford, Diego de Las Casas, Lisa Anne Hendricks, Johannes Welbl, Aidan Clark, Tom Hennigan, Eric Noland, Katie Millican, George van den Driessche, Bogdan Damoc, Aurelia Guy, Simon Osindero, Karen Simonyan, Erich Elsen, Jack W. Rae, Oriol Vinyals, and L. Sifre. Training compute-optimal large language models. *ArXiv*, abs/2203.15556, 2022.
- [49] Fan Bao, Shen Nie, Kaiwen Xue, Yue Cao, Chongxuan Li, Hang Su, and Jun Zhu. All are worth words: A vit backbone for diffusion models. In *Proceedings of the IEEE/CVF Conference on Computer Vision and Pattern Recognition*, pages 22669–22679, 2023.
- [50] William Peebles and Saining Xie. Scalable diffusion models with transformers. In *Proceedings of the IEEE/CVF International Conference on Computer Vision*, pages 4195–4205, 2023.
- [51] Fan Bao, Shen Nie, Kaiwen Xue, Chongxuan Li, Shiliang Pu, Yaole Wang, Gang Yue, Yue Cao, Hang Su, and Jun Zhu. One transformer fits all distributions in multi-modal diffusion at scale. In *International Conference on Machine Learning*, 2023.
- [52] Fan Bao, Chendong Xiang, Gang Yue, Guande He, Hongzhou Zhu, Kaiwen Zheng, Min Zhao, Shilong Liu, Yaole Wang, and Jun Zhu. Vidu: a highly consistent, dynamic and skilled text-to-video generator with diffusion models. *arXiv preprint arXiv:2405.04233*, 2024.
- [53] Ashish Vaswani, Noam M. Shazeer, Niki Parmar, Jakob Uszkoreit, Llion Jones, Aidan N. Gomez, Lukasz Kaiser, and Illia Polosukhin. Attention is all you need. In *Neural Information Processing Systems*, 2017.
- [54] Jacob Devlin, Ming-Wei Chang, Kenton Lee, and Kristina Toutanova. BERT: Pre-training of deep bidirectional transformers for language understanding. In *Proceedings of the 2019 Conference of the North American Chapter of the Association for Computational Linguistics: Human Language Technologies, Volume 1 (Long and Short Papers)*. Association for Computational Linguistics, 2019.
- [55] Jianlin Su, Yu Lu, Shengfeng Pan, Bo Wen, and Yunfeng Liu. Roformer: Enhanced transformer with rotary position embedding. *Neurocomputing*, 2021.
- [56] William S. Peebles and Saining Xie. Scalable diffusion models with transformers. In *International Conference on Computer Vision*, 2023.

A Detailed Notations and Definitions

- x, \hat{x} : Scalar variables representing states in a model.
- \mathcal{X} : A one-dimensional sample space $\{1, \dots, N\}$.
- \mathbf{Q}_t : The transition rate matrix at time t .
- p : The probability of the forward process defined by the transition rate matrix \mathbf{Q}_t .
- q_θ : The probability of the reverse process defined by model c_θ .
- $p_{t|s}(\hat{x}|x)$: The transition probability from state x to state \hat{x} from time s to time t .
- $p_t(x)$: The probability of x at time t .
- $\mathbf{P}_{t|s}$: The transition probability matrix from time s to time t .
- $\sigma(t)$: The noise schedule function.
- $\tilde{\mathbf{Q}}_t$: The reverse transition rate matrix at time t .
- $s_\theta(\mathbf{x}_t, t)_{\hat{x}_t}$: The corresponding element of $s_\theta(\mathbf{x}_t, t)$, which approximates $\frac{p_t(\hat{x}_t)}{p_t(\mathbf{x})}$.
- $[\mathbf{M}]$: A special mask token in the absorbing process.
- \mathcal{X}^d : A multi-dimensional sample space $\{1, \dots, N\}^d$.
- \mathbf{x}_t : A multi-dimensional vector.
- x_t^i : The i -th element of \mathbf{x}_t .
- $p_{s|t}^i(\cdot|\mathbf{x}_t)$: The probability on dimension i from time s to time t conditioned on full vector \mathbf{x}_t .
- $p_{s|t}^{\text{tweedie}}(\cdot|\cdot)$: The transition probability from time s to time t under Tweedie τ -leaping method.
- $p_{s|t}^{\text{euler}}(\cdot|\cdot)$: The transition probability from time s to time t under the Euler method.
- $\mathbf{Q}_t^{\text{tok}}$: Transition rate matrix for each dimension of \mathbf{x}_t .
- \mathbf{x}^{UM} : vector consists of all unmasked tokens of \mathbf{x} .
- $\mathbf{x}^{a:b}$: The elements of \mathbf{x} with indices ranging from a to b .
- $c_\theta(\mathbf{x}_t)$: A network that characterizes the time-independent conditional probabilities in reparameterized absorbing discrete diffusion (RADD).
- d : Total sequence length or dimension of \mathbf{x} .
- l : Generating sequence length.
- π : one permutation, $\pi(l)$ denotes the l -th element of permutation π , $\pi(< l)$ denotes the elements of permutation π with indices less than l .
- $U(\cdot)$: Uniform distribution.
- $p_\lambda(\cdot|\mathbf{x}_0)$: The joint distribution induced by masking each dimension in \mathbf{x}_0 independently with a probability λ .
- Cat: Categorical distribution.
- NFEs: Number of function evaluations.
- E-NFEs: Expected number of function evaluations.

B Proof of Theorem 1

In this section, we provide a detailed proof of Theorem 1, which is carried out in three key steps. The core idea of the proof involves leveraging the properties of a continuous-time Markov chain with an absorbing state, where the forward diffusion process is independent across different dimensions. This independence simplifies the analysis of both the conditional and joint distributions.

First, we derive the analytic form of the conditional distribution, as stated in Lemma 1. This can be derived directly from Eq. (2.3), but for a better understanding, we provide a more intuitive proof

for $\mathbf{Q}_t = \sigma(t)\mathbf{Q}^{\text{absorb}}$. Second, we extend this analysis to multiple dimensions to obtain the joint distribution, as formalized in Proposition 1. Finally, by simply dividing the joint distributions derived in the second step, we decouple the concrete score, thereby completing the proof of Theorem 1.

Lemma 1. *(Analytic conditional distribution in absorbing diffusion) Suppose $\{X_t\}$ is a continuous time Markov chain with transition rate matrix $\mathbf{Q}_t = \sigma(t)\mathbf{Q}^{\text{absorb}}$, given the value x_0 at time zero, the conditional distribution $p_{t|0}(x_t|x_0)$ has the following analytic form:*

$$p_{t|0}(x_t|x_0) = \begin{cases} e^{-\bar{\sigma}(t)}, & x_t = x_0, \\ 1 - e^{-\bar{\sigma}(t)}, & x_t = [\mathbf{M}], \\ 0, & x_t \neq [\mathbf{M}] \text{ and } x_t \neq x_0. \end{cases} \quad (\text{B.1})$$

Proof. Given the initial value $x_0 \in \mathcal{X} = \{1, \dots, N\}$, we have

$$x_t = \begin{cases} x_0, & t < T_h, \\ [\mathbf{M}], & t \geq T_h. \end{cases} \quad (\text{B.2})$$

Here, T_h represents the holding time before x_0 transitions to the absorbing state $[\mathbf{M}]$.

Based on the definition of the \mathbf{Q}_t in Eq. (2.2) and $\mathbf{Q}^{\text{absorb}}$, the probability of x_0 remaining the same after a small time increment Δt is

$$p_{t+\Delta t|t}(x_0|x_0) = 1 + \sigma(t)\mathbf{Q}^{\text{absorb}}(x_0, x_0)\Delta t + o(\Delta t). \quad (\text{B.3})$$

Partitioning the interval $[0, t]$ into $\{s_k\}_{k=0}^n$ and utilizing the memoryless property of continuous-time Markov chains, we can express the probability of x_0 remaining the same from time 0 to t as a product of probabilities over these small intervals. This gives us:

$$p_{t|0}(x_0|x_0) = \prod_{k=1}^n p_{s_k|s_{k-1}}(x_0|x_0) \quad (\text{B.4})$$

$$= \prod_{k=1}^n (1 + \sigma(t_{k-1})\mathbf{Q}^{\text{absorb}}(x_0, x_0)(s_k - s_{k-1}) + o(s_k - s_{k-1})) \quad (\text{B.5})$$

$$= \exp\left(\sum_{k=1}^n \ln(1 + \sigma(t_{k-1})\mathbf{Q}^{\text{absorb}}(x_0, x_0)(s_k - s_{k-1}) + o(s_k - s_{k-1}))\right) \quad (\text{B.6})$$

$$= \exp\left(\sum_{k=1}^n \sigma(t_{k-1})\mathbf{Q}^{\text{absorb}}(x_0, x_0)(s_k - s_{k-1}) + o(s_k - s_{k-1})\right). \quad (\text{B.7})$$

Let $\max(s_k - s_{k-1}) \rightarrow 0$, the Riemann sum in Eq. (B.7) equals the following continuous integral:

$$p_{t|0}(x_0|x_0) = \exp\left(\int_0^t \sigma(s)\mathbf{Q}^{\text{absorb}}(x_0, x_0)ds\right) = \exp(\mathbf{Q}^{\text{absorb}}(x_0, x_0)\bar{\sigma}(t)). \quad (\text{B.8})$$

By Eq. (2.4), $\mathbf{Q}^{\text{absorb}}(x_0, x_0) = -1$, we have

$$p_{t|0}(x_0|x_0) = P(T_h > t) = e^{-\bar{\sigma}(t)} \quad (\text{B.9})$$

$$p_{t|0}([\mathbf{M}]|x_0) = P(T_h \leq t) = 1 - e^{-\bar{\sigma}(t)} \quad (\text{B.10})$$

$$p_{t|0}(k|x_0) = 0 \quad \text{if } k \neq [\mathbf{M}] \text{ and } k \neq x_0. \quad (\text{B.11})$$

Similarly, given value x_s at time $s < t$, the conditional distribution can be expressed as

$$p_{t|s}(x_t|x_s) = \begin{cases} e^{-(\bar{\sigma}(t)-\bar{\sigma}(s))}, & x_t = x_s, \\ 1 - e^{-(\bar{\sigma}(t)-\bar{\sigma}(s))}, & x_t = [\mathbf{M}], \\ 0, & x_t \neq [\mathbf{M}] \text{ and } x_t \neq x_s. \end{cases} \quad (\text{B.12})$$

□

Proposition 1. (Analytic joint distribution in absorbing diffusion)

Suppose $\{X_t\}$ is a continuous time Markov chain with transition rate matrix $\mathbf{Q}_t = \sigma(t)\mathbf{Q}^{absorb}$. For $\mathbf{x}_t = x_t^1 \cdots x_t^d$ with d_1 components as $[\mathbf{M}]$ and $d_2 = d - d_1$ components as unmasked tokens, $p_t(\mathbf{x}_t)$ can be expressed as

$$p_t(\mathbf{x}_t) = [1 - e^{-\bar{\sigma}(t)}]^{d_1} [e^{-\bar{\sigma}(t)}]^{d_2} p_0(\mathbf{x}_t^{UM}), \quad (\text{B.13})$$

where \mathbf{x}_t^{UM} is the vector consists of all unmasked tokens of \mathbf{x}_t .

Proposition 1 shows that the joint distribution $p_t(\mathbf{x}_t)$ can be expressed as the multiplication of two terms. One is an analytic term only depending on time, the other is a d_2 dimensions joint distribution of clean data $p_0(\mathbf{x}_t^{UM})$ independent of time.

Proof. Without loss of generality, let's assume that the preceding d_1 terms of \mathbf{x} are all $[\mathbf{M}]$, and the remaining d_2 terms are unmasked tokens. That is, $\mathbf{x}_t = [\mathbf{M}] \cdots [\mathbf{M}]x_t^{d_1+1} \cdots x_t^d$, and here x^k is an unmasked token in \mathcal{X} .

Using the law of total probability and Lemma 1, along with the assumption of independence between different dimensions of the diffusion process, we can express the joint distribution $p_t([\mathbf{M}] \cdots [\mathbf{M}]x_t^{d_1+1} \cdots x_t^d)$ as a sum over all possible initial states $\mathbf{x}_0 \in \mathcal{X}^d$:

$$\begin{aligned} p_t([\mathbf{M}] \cdots [\mathbf{M}]x_t^{d_1+1} \cdots x_t^d) &= \sum_{\mathbf{x}_0 \in \mathcal{X}^d} p_{t|0}([\mathbf{M}] \cdots [\mathbf{M}]x_t^{d_1+1} \cdots x_t^d | \mathbf{x}_0) p_0(\mathbf{x}_0) \\ &= \sum_{x_0^1 \in \mathcal{X}, \dots, x_0^d \in \mathcal{X}} p_{t|0}([\mathbf{M}] \cdots [\mathbf{M}]x_t^{d_1+1} \cdots x_t^d | x_0^1 \cdots x_0^d) p_0(x_0^1 \cdots x_0^d) \\ &= \sum_{x_0^1 \in \mathcal{X}, \dots, x_0^d \in \mathcal{X}} \prod_{k=1}^{d_1} p_{t|0}^k([\mathbf{M}] | x_0^k) \prod_{k=d_1+1}^d p_{t|0}^k(x_t^k | x_0^k) p_0(x_0^1 \cdots x_0^d). \end{aligned}$$

Substituting the analytic forms of $p_{t|0}^k([\mathbf{M}] | x_0^k)$ and $p_{t|0}^k(x_t^k | x_0^k)$ from Lemma 1, above equations can be further simplified as follows:

$$\begin{aligned} &\sum_{x_0^1 \in \mathcal{X}, \dots, x_0^d \in \mathcal{X}} \prod_{k=1}^{d_1} p_{t|0}^k([\mathbf{M}] | x_0^k) \prod_{k=d_1+1}^d p_{t|0}^k(x_t^k | x_0^k) p_0(x_0^1 \cdots x_0^d) \\ &= \sum_{x_0^1 \in \mathcal{X}, \dots, x_0^{d_1} \in \mathcal{X}} \prod_{k=1}^{d_1} p_{t|0}^k([\mathbf{M}] | x_0^k) [e^{-\bar{\sigma}(t)}]^{d_2} p_0(x_0^1 \cdots x_0^{d_1} x_t^{d_1+1} \cdots x_t^d) \\ &= \sum_{x_0^1 \in \mathcal{X}, \dots, x_0^{d_1} \in \mathcal{X}} [1 - e^{-\bar{\sigma}(t)}]^{d_1} [e^{-\bar{\sigma}(t)}]^{d_2} p_0(x_0^1 \cdots x_0^{d_1} x_t^{d_1+1} \cdots x_t^d) \\ &= [1 - e^{-\bar{\sigma}(t)}]^{d_1} [e^{-\bar{\sigma}(t)}]^{d_2} \sum_{x_0^1 \in \mathcal{X}, \dots, x_0^{d_1} \in \mathcal{X}} p_0(x_0^1 \cdots x_0^{d_1} x_t^{d_1+1} \cdots x_t^d) \\ &= [1 - e^{-\bar{\sigma}(t)}]^{d_1} [e^{-\bar{\sigma}(t)}]^{d_2} p_0(x_t^{d_1+1} \cdots x_t^d). \end{aligned}$$

By noting that $p_0(x_t^{d_1+1} \cdots x_t^d) = p_0(\mathbf{x}_t^{UM})$, in the general case, we have

$$p_t(\mathbf{x}_t) = [1 - e^{-\bar{\sigma}(t)}]^{d_1} [e^{-\bar{\sigma}(t)}]^{d_2} p_0(\mathbf{x}_t^{UM}),$$

which demonstrates that the likelihood of the noisy data \mathbf{x}_t at time t equals the likelihood of the unmasked part \mathbf{x}_t^{UM} at time 0 multiplied by an analytic time-dependent term. \square

Theorem 1. (Analytic concrete score in absorbing diffusion, proof in Appendix B) For $\mathbf{x}_t = x_t^1 \cdots x_t^i \cdots x_t^d$ and $\hat{\mathbf{x}}_t = x_t^1 \cdots \hat{x}_t^i \cdots x_t^d$, if $x_t^i = [\mathbf{M}]$ and $\hat{x}_t^i \neq [\mathbf{M}]$, the concrete score at time t can be expressed as a **time-independent** conditional distribution at time zero multiplied by an analytic **time-dependent** term:

$$\frac{p_t(x_t^1 \cdots \hat{x}_t^i \cdots x_t^d)}{p_t(x_t^1 \cdots x_t^i \cdots x_t^d)} = \frac{e^{-\bar{\sigma}(t)}}{1 - e^{-\bar{\sigma}(t)}} p_0(\hat{x}_t^i | \mathbf{x}_t^{UM}),$$

where \mathbf{x}_t^{UM} is the vector consists of all unmasked tokens of \mathbf{x}_t .

Proof. According to Proposition 1, if $x_t^i = [\mathbf{M}]$ and $\hat{x}_t^i \neq [\mathbf{M}]$, $\hat{\mathbf{x}}_t^{UM} = (\mathbf{x}_t^{UM}, \hat{x}_t^i)$,

$$\begin{aligned} \frac{p_t(\hat{\mathbf{x}}_t)}{p_t(\mathbf{x}_t)} &= \frac{[1 - e^{-\bar{\sigma}(t)}]^{d_1-1} [e^{-\bar{\sigma}(t)}]^{d_2+1} p_0(\hat{\mathbf{x}}_t^{UM})}{[1 - e^{-\bar{\sigma}(t)}]^{d_1} [e^{-\bar{\sigma}(t)}]^{d_2} p_0(\mathbf{x}_t^{UM})} \\ &= \frac{[1 - e^{-\bar{\sigma}(t)}]^{d_1-1} [e^{-\bar{\sigma}(t)}]^{d_2+1} p_0(\mathbf{x}_t^{UM}, \hat{x}_t^i)}{[1 - e^{-\bar{\sigma}(t)}]^{d_1} [e^{-\bar{\sigma}(t)}]^{d_2} p_0(\mathbf{x}_t^{UM})} \\ &= \frac{e^{-\bar{\sigma}(t)}}{1 - e^{-\bar{\sigma}(t)}} p_0(\hat{x}_t^i | \mathbf{x}_t^{UM}). \end{aligned}$$

□

C Proof of Theorem 2

Theorem 2. *The absorbing discrete diffusion objective of Eq. (2.6) is equivalent to any-order autoregressive objective of Eq. (2.11) when the final total noise level $\bar{\sigma}(T) \rightarrow +\infty$.*

Here, the infinity final total noise level guarantees that all tokens will be finally masked with probability one ($1 - e^{-\bar{\sigma}(T)}$). Below we present the detailed proof in three steps.

C.1 Equivalence between DSE loss and t-DCE loss

For a given noisy input \mathbf{x}_t , as established in Section 3.1, $\hat{\mathbf{x}}_t$ is valid only when it contains exactly one more unmasked token than \mathbf{x}_t . In this case, the transition probability $\mathbf{Q}_t(\hat{\mathbf{x}}_t, \mathbf{x}_t)$ equals $\sigma(t)$.

Replace $s_\theta(\mathbf{x}_t)$ with $\frac{e^{-\bar{\sigma}(t)}}{1 - e^{-\bar{\sigma}(t)}} \mathbf{c}_\theta(\mathbf{x}_t)$, we can express the DSE loss in the multi-dimensional case as follows:

$$\begin{aligned} \mathcal{L}_{\text{DSE}}^T(\mathbf{x}_0) &= \int_0^T \mathbb{E}_{\mathbf{x}_t \sim p_{t|0}(\mathbf{x}_t | \mathbf{x}_0)} \left[\sum_{x_t^i = [\mathbf{M}], j \neq [\mathbf{M}]} \sigma(t) \left(\frac{e^{-\bar{\sigma}(t)}}{1 - e^{-\bar{\sigma}(t)}} \mathbf{c}_\theta(\mathbf{x}_t)[i, j] \right. \right. \\ &\quad \left. \left. - \frac{e^{-\bar{\sigma}(t)}}{1 - e^{-\bar{\sigma}(t)}} \mathbb{I}(x_0^i = j) \log \left(\frac{e^{-\bar{\sigma}(t)}}{1 - e^{-\bar{\sigma}(t)}} \mathbf{c}_\theta(\mathbf{x}_t)[i, j] \right) + K \left(\frac{e^{-\bar{\sigma}(t)}}{1 - e^{-\bar{\sigma}(t)}} I(x_0^i = j) \right) \right) \right] dt \\ &= \int_0^T \mathbb{E}_{\mathbf{x}_t \sim p_{t|0}(\mathbf{x}_t | \mathbf{x}_0)} \left[\sum_{x_t^i = [\mathbf{M}], j \neq [\mathbf{M}]} \sigma(t) \left(\frac{e^{-\bar{\sigma}(t)}}{1 - e^{-\bar{\sigma}(t)}} \mathbf{c}_\theta(\mathbf{x}_t)[i, j] \right) \right] dt \\ &\quad + \int_0^T \mathbb{E}_{\mathbf{x}_t \sim p_{t|0}(\mathbf{x}_t | \mathbf{x}_0)} \left[\sum_{x_t^i = [\mathbf{M}], j \neq [\mathbf{M}]} \left(-\frac{\sigma(t) e^{-\bar{\sigma}(t)}}{1 - e^{-\bar{\sigma}(t)}} \mathbb{I}(x_0^i = j) \log \left(\frac{e^{-\bar{\sigma}(t)}}{1 - e^{-\bar{\sigma}(t)}} \mathbf{c}_\theta(\mathbf{x}_t)[i, j] \right) \right) \right] dt \\ &\quad + \int_0^T \mathbb{E}_{\mathbf{x}_t \sim p_{t|0}(\mathbf{x}_t | \mathbf{x}_0)} \left[\sum_{x_t^i = [\mathbf{M}], j \neq [\mathbf{M}]} \sigma(t) K \left(\frac{e^{-\bar{\sigma}(t)}}{1 - e^{-\bar{\sigma}(t)}} I(x_0^i = j) \right) \right] dt. \end{aligned}$$

We analyze each term in the above equation separately. The first term simplifies due to the property $\sum_{j \neq [\mathbf{M}]} \mathbf{c}_\theta(\mathbf{x}_t)[i, j] = 1$:

$$\int_0^T \mathbb{E}_{\mathbf{x}_t \sim p_{t|0}(\mathbf{x}_t | \mathbf{x}_0)} \left[\sum_{x_t^i = [\mathbf{M}]} \sigma(t) \frac{e^{-\bar{\sigma}(t)}}{1 - e^{-\bar{\sigma}(t)}} \right] dt. \quad (\text{C.1})$$

The third term can be simplified by substituting $K(a) = a \log a - a$ and using $0 \log 0 = 0$:

$$\int_0^T \mathbb{E}_{\mathbf{x}_t \sim p_{t|0}(\mathbf{x}_t | \mathbf{x}_0)} \left[\sum_{x_t^i = [\mathbf{M}]} \sigma(t) \frac{e^{-\bar{\sigma}(t)}}{1 - e^{-\bar{\sigma}(t)}} \left(\log \frac{e^{-\bar{\sigma}(t)}}{1 - e^{-\bar{\sigma}(t)}} - 1 \right) \right] dt. \quad (\text{C.2})$$

Combining the first and third terms:

$$\int_0^T \mathbb{E}_{\mathbf{x}_t \sim p_{t|0}(\mathbf{x}_t|\mathbf{x}_0)} \left[\sum_{x_t^i = [\mathbf{M}]} \sigma(t) \frac{e^{-\bar{\sigma}(t)}}{1 - e^{-\bar{\sigma}(t)}} \left(\log \frac{e^{-\bar{\sigma}(t)}}{1 - e^{-\bar{\sigma}(t)}} \right) \right] dt \quad (\text{C.3})$$

$$= \int_0^T d(1 - e^{-\bar{\sigma}(t)}) \sigma(t) \frac{e^{-\bar{\sigma}(t)}}{1 - e^{-\bar{\sigma}(t)}} \left(\log \frac{e^{-\bar{\sigma}(t)}}{1 - e^{-\bar{\sigma}(t)}} \right) dt \quad (\text{C.4})$$

$$= d \int_0^T \sigma(t) e^{-\bar{\sigma}(t)} \log \frac{e^{-\bar{\sigma}(t)}}{1 - e^{-\bar{\sigma}(t)}} dt. \quad (\text{C.5})$$

Introducing a new variable $\lambda(t) = 1 - e^{-\bar{\sigma}(t)}$, which represents the probability of a token being masked from 0 to t in the forward process. As $\bar{\sigma}(t) = \int_0^t \sigma(\tau) d\tau$ and $\bar{\sigma}(T) = \infty$, we have $\lambda(0) = 0$, $\lambda(T) = 1$ and $d\lambda = \sigma(t) e^{-\bar{\sigma}(t)} dt$. Obviously, $\lambda(t)$ is invertible, which allows us to perform a change of variables from t to λ and simplifies Eq. (C.5) to

$$d \int_0^1 \log \frac{1 - \lambda}{\lambda} d\lambda = -d(\lambda \log \lambda + (1 - \lambda) \log(1 - \lambda)) \Big|_0^1 = 0. \quad (\text{C.6})$$

Here we used

$$\lim_{\lambda \rightarrow 0} \lambda \log \lambda = \lim_{\lambda \rightarrow 1} (1 - \lambda) \log(1 - \lambda) = 0.$$

Thus, the DSE loss reduces to the second term, which we define as the t -denoising cross-entropy loss (t -DCE):

$$\begin{aligned} \mathcal{L}_{t\text{-DCE}}^T(\mathbf{x}_0) &= \int_0^T \mathbb{E}_{\mathbf{x}_t \sim p_{t|0}(\mathbf{x}_t|\mathbf{x}_0)} \left[\sum_{x_t^i = [\mathbf{M}], j \neq [\mathbf{M}]} -\frac{\sigma(t) e^{-\bar{\sigma}(t)}}{1 - e^{-\bar{\sigma}(t)}} \mathbb{I}(x_0^i = j) \log \left(\frac{e^{-\bar{\sigma}(t)}}{1 - e^{-\bar{\sigma}(t)}} \mathbf{c}_\theta(\mathbf{x}_t)[i, j] \right) \right] dt \\ &= \int_0^T \mathbb{E}_{\mathbf{x}_t \sim p_{t|0}(\mathbf{x}_t|\mathbf{x}_0)} \left[\sum_{x_t^i = [\mathbf{M}]} -\frac{\sigma(t) e^{-\bar{\sigma}(t)}}{1 - e^{-\bar{\sigma}(t)}} \log \left(\frac{e^{-\bar{\sigma}(t)}}{1 - e^{-\bar{\sigma}(t)}} \mathbf{c}_\theta(\mathbf{x}_t)[i, x_0^i] \right) \right] dt \\ &= \int_0^T \mathbb{E}_{\mathbf{x}_t \sim p_{t|0}(\mathbf{x}_t|\mathbf{x}_0)} \left[\sum_{x_t^i = [\mathbf{M}]} -\frac{\sigma(t) e^{-\bar{\sigma}(t)}}{1 - e^{-\bar{\sigma}(t)}} \log \left(\frac{e^{-\bar{\sigma}(t)}}{1 - e^{-\bar{\sigma}(t)}} q_\theta(x_0^i | \mathbf{x}_t^{\text{UM}}) \right) \right] dt. \end{aligned}$$

C.2 Equivalence between t -DCE loss and lambda-DCE loss

Starting from the t -DCE loss in Eq. (3.4), we can perform a change of variable from t to $\lambda(t) = 1 - e^{-\bar{\sigma}(t)}$, as demonstrated in Appendix C.1. This allows us to rewrite the t -DCE loss integral in terms of λ :

$$\begin{aligned} &\int_0^1 \frac{1}{\lambda} \mathbb{E}_{\mathbf{x}_\lambda \sim p_\lambda(\mathbf{x}_\lambda|\mathbf{x}_0)} \left[\sum_{x_\lambda^i = [\mathbf{M}]} -\log \left(\frac{1 - \lambda}{\lambda} q_\theta(x_0^i | \mathbf{x}_\lambda^{\text{UM}}) \right) \right] d\lambda \\ &= \int_0^1 \frac{1}{\lambda} \mathbb{E}_{\mathbf{x}_\lambda \sim p_\lambda(\mathbf{x}_\lambda|\mathbf{x}_0)} \left[\sum_{x_\lambda^i = [\mathbf{M}]} -\log q_\theta(x_0^i | \mathbf{x}_\lambda^{\text{UM}}) \right] d\lambda + \int_0^1 \frac{1}{\lambda} \mathbb{E}_{\mathbf{x}_\lambda \sim p_\lambda(\mathbf{x}_\lambda|\mathbf{x}_0)} \left[\sum_{x_\lambda^i = [\mathbf{M}]} -\log \left(\frac{1 - \lambda}{\lambda} \right) \right] d\lambda. \end{aligned}$$

Given the independence of the forward process and Lemma 1, the original probability $p_{t|0}(\mathbf{x}_t|\mathbf{x}_0)$ can be factorized as $\prod_{i=1}^d p_{t|0}^i(x_t^i|x_0^i)$, where

$$p_{t|0}^i(x_t^i|x_0^i) = \begin{cases} 1 - e^{-\bar{\sigma}(t)}, & x_t^i = [\mathbf{M}], \\ e^{-\bar{\sigma}(t)}, & x_t^i = x_0^i, \\ 0, & \text{else.} \end{cases} \quad (\text{C.7})$$

Therefore, the induced probability $p_\lambda(\mathbf{x}_\lambda|\mathbf{x}_0) = \prod_{i=1}^d p_\lambda^i(x_\lambda^i|x_0^i)$ where

$$p_\lambda^i(x_\lambda^i|x_0^i) = \begin{cases} \lambda, & x_\lambda^i = [\mathbf{M}], \\ 1 - \lambda, & x_\lambda^i = x_0^i, \\ 0, & \text{else.} \end{cases} \quad (\text{C.8})$$

Next, consider the second term in the λ integral. Similar to Eq. (C.3), we can prove that it equals zero:

$$\int_0^1 \frac{1}{\lambda} \mathbb{E}_{\mathbf{x}_\lambda \sim p_\lambda(\mathbf{x}_\lambda | \mathbf{x}_0)} \left[\sum_{x_\lambda^i = [\mathbf{M}]} -\log\left(\frac{1-\lambda}{\lambda}\right) \right] = 0. \quad (\text{C.9})$$

Therefore, t -DCE loss is equivalent to the first term, which we defined as λ -denoising cross-entropy (λ -DCE):

$$\mathcal{L}_{\lambda\text{-DCE}}^T(\mathbf{x}_0) = \int_0^1 \frac{1}{\lambda} \mathbb{E}_{\mathbf{x}_\lambda \sim p_\lambda(\mathbf{x}_\lambda | \mathbf{x}_0)} \left[\sum_{x_\lambda^i = [\mathbf{M}]} -\log q_\theta(x_0^i | \mathbf{x}_\lambda^{\text{UM}}) \right] d\lambda. \quad (\text{C.10})$$

C.3 Equivalence between lambda-DCE loss and any-order autoregressive loss

Based on λ -DCE loss in Eq. (3.5), we first define the sample space and analytically express the expectation term.

Given \mathbf{x}_0 , we define the sample space of \mathbf{x}_λ as $\tilde{\mathcal{X}}(\mathbf{x}_0) := \{x_0^1, [\mathbf{M}]\} \times \cdots \times \{x_0^d, [\mathbf{M}]\}$ and $\tilde{\mathcal{X}}_k(\mathbf{x}_0) := \{\tilde{\mathbf{x}} : \tilde{\mathbf{x}} \in \tilde{\mathcal{X}}(\mathbf{x}_0) \wedge \tilde{\mathbf{x}}$ has exact k dimensions with values $[\mathbf{M}]\}$. It follows that $|\tilde{\mathcal{X}}(\mathbf{x}_0)| = 2^d$ and $|\tilde{\mathcal{X}}_k(\mathbf{x}_0)| = \binom{d}{k}$. Therefore, the sample space $\tilde{\mathcal{X}}(\mathbf{x}_0)$ can be decoupled by the number of masked tokens k in $\tilde{\mathbf{x}}$:

$$\int_0^1 \frac{1}{\lambda} \mathbb{E}_{\mathbf{x}_\lambda \sim p_\lambda(\mathbf{x}_\lambda | \mathbf{x}_0)} \left[\sum_{\tilde{\mathbf{x}}^i = [\mathbf{M}]} -\log q_\theta(x_0^i | \mathbf{x}_\lambda^{\text{UM}}) \right] d\lambda \quad (\text{C.11})$$

$$= \int_0^1 \frac{1}{\lambda} \sum_{\tilde{\mathbf{x}} \in \tilde{\mathcal{X}}(\mathbf{x}_0)} p_\lambda(\tilde{\mathbf{x}} | \mathbf{x}_0) \left[\sum_{\tilde{\mathbf{x}}^i = [\mathbf{M}]} -\log q_\theta(x_0^i | \tilde{\mathbf{x}}^{\text{UM}}) \right] d\lambda \quad (\text{C.12})$$

$$= \int_0^1 \frac{1}{\lambda} \sum_{k=0}^d \sum_{\tilde{\mathbf{x}} \in \tilde{\mathcal{X}}_k(\mathbf{x}_0)} \lambda^k (1-\lambda)^{d-k} \left[\sum_{\tilde{\mathbf{x}}^i = [\mathbf{M}]} -\log q_\theta(x_0^i | \tilde{\mathbf{x}}^{\text{UM}}) \right] d\lambda \quad (\text{C.13})$$

$$= \int_0^1 \frac{1}{\lambda} \sum_{k=1}^d \sum_{\tilde{\mathbf{x}} \in \tilde{\mathcal{X}}_k(\mathbf{x}_0)} \lambda^k (1-\lambda)^{d-k} \left[\sum_{\tilde{\mathbf{x}}^i = [\mathbf{M}]} -\log q_\theta(x_0^i | \tilde{\mathbf{x}}^{\text{UM}}) \right] d\lambda. \quad (\text{C.14})$$

The last equation holds because there are no masked tokens when $k = 0$, and the inner sum is zero.

From Eq. (C.14), by rearranging the order of summation and integration, we can analytically evaluate the integral $\int_0^1 \lambda^{k-1} (1-\lambda)^{d-k} d\lambda$ using the Beta function, which eliminates λ :

$$\text{Eq. (C.14)} = \sum_{k=1}^d \int_0^1 \lambda^{k-1} (1-\lambda)^{d-k} d\lambda \sum_{\tilde{\mathbf{x}} \in \tilde{\mathcal{X}}_k(\mathbf{x}_0)} \left[\sum_{\tilde{\mathbf{x}}^i = [\mathbf{M}]} -\log q_\theta(x_0^i | \tilde{\mathbf{x}}^{\text{UM}}) \right] \quad (\text{C.15})$$

$$= \sum_{k=1}^d \frac{(k-1)!(d-k)!}{d!} \sum_{\tilde{\mathbf{x}} \in \tilde{\mathcal{X}}_k(\mathbf{x}_0)} \left[\sum_{\tilde{\mathbf{x}}^i = [\mathbf{M}]} -\log q_\theta(x_0^i | \tilde{\mathbf{x}}^{\text{UM}}) \right] \quad (\text{C.16})$$

$$= \sum_{k=1}^d \frac{1}{k \binom{d}{k}} \sum_{\tilde{\mathbf{x}} \in \tilde{\mathcal{X}}_k(\mathbf{x}_0)} \left[\sum_{\tilde{\mathbf{x}}^i = [\mathbf{M}]} -\log q_\theta(x_0^i | \tilde{\mathbf{x}}^{\text{UM}}) \right]. \quad (\text{C.17})$$

Eq. (C.17) can be reformulated in terms of an expectation over a uniform distribution $U(\tilde{\mathcal{X}}_k(\mathbf{x}_0))$ as follows:

$$\sum_{k=1}^d \frac{1}{k} \mathbb{E}_{\tilde{\mathbf{x}} \sim U(\tilde{\mathcal{X}}_k(\mathbf{x}_0))} \left[\sum_{\tilde{\mathbf{x}}^i = [\mathbf{M}]} (-\log(q_\theta(x_0^i | \tilde{\mathbf{x}}^{\text{UM}})) \right]. \quad (\text{C.18})$$

Let π be one permutation of the integers $1, \dots, d$, and U_π represent the uniform distribution of all orders. We note that Eq. (C.18) is equivalent to the following term from the perspective of any-order autoregressive model:

$$\sum_{k=1}^d \frac{1}{k} \mathbb{E}_{\pi \sim U_\pi} \sum_{r=d-k+1}^d -\log q_\theta(x_0^{\pi(r)} | x_0^{\pi(<d-k+1)}; \pi). \quad (\text{C.19})$$

Here, $x_0^{\pi(<l)}$ denotes the sequence of the first $l-1$ elements in the permutation π . Given a fixed k , the term $x_0^{\pi(<d-k+1)}$ can be interpreted as the unmasked part of the noisy data $\tilde{\mathbf{x}}^{\text{UM}}$. For $r = d-k+1, \dots, d$, $x_0^{\pi(r)}$ corresponds to the k items of the masked part. Since both π and $\tilde{\mathbf{x}}$ are both uniformly sampled, Eq. (C.18) and Eq. (C.19) are equivalent.

Further, we can make a simple subscription transformation by letting $l = d - k + 1$ and change the summation to Monte Carlo estimation on Eq. (C.19) :

$$d \cdot \mathbb{E}_{l \sim U(1, \dots, d)} \frac{1}{d-l+1} \mathbb{E}_{\pi \sim U_\pi} \sum_{r=l}^d -\log q_\theta(x_0^{\pi(r)} | x_0^{\pi(<l)}; \pi). \quad (\text{C.20})$$

In [30, 31], it was proved that Eq. (C.20) is mathematically equivalent to Eq. (2.11). Actually, Eq. (C.20) is widely used as a training objective for any-order autoregressive models for efficient parallel optimization.

This concludes our proof of Theorem 2.

D Sampling methods

In this section, we first derived the exact reverse distribution for absorbing discrete diffusion in Appendix D.1. This derivation led to simplified forms of the Tweedie τ -leaping and Euler methods, detailed in Appendix D.2 and Appendix D.3, respectively. In Appendix D.4, we proved the equivalence of these two methods under a log-linear noise schedule. Finally, in Appendix D.5, we discussed the expected number of function evaluations (E-NFEs) for these methods.

D.1 Exact reverse distribution in absorbing discrete diffusion

Lemma 2. (Analytic reverse distribution in absorbing diffusion) Suppose $\{X_t\}$ is a continuous time Markov chain with transition rate matrix $\mathbf{Q}_t = \sigma(t)\mathbf{Q}^{\text{absorb}}$. For $\mathbf{x}_t = x_t^1 \dots x_t^d$ with d_1 masked tokens and $d_2 = d - d_1$ unmasked tokens, and $\mathbf{x}_s = x_s^1 \dots x_s^d$ with $d_1 - \Delta d$ masked tokens and $d_2 + \Delta d$ unmasked tokens, the reverse distribution is given by:

$$p_{s|t}(\mathbf{x}_s | \mathbf{x}_t) = \begin{cases} \left[\frac{e^{-\bar{\sigma}(s)} - e^{-\bar{\sigma}(t)}}{1 - e^{-\bar{\sigma}(s)}} \right]^{\Delta d} \left[\frac{1 - e^{-\bar{\sigma}(s)}}{1 - e^{-\bar{\sigma}(t)}} \right]^{d_1} \frac{p_0(\mathbf{x}_s^{\text{UM}})}{p_0(\mathbf{x}_t^{\text{UM}})}, & \mathbf{x}_t \subseteq_{\text{UM}} \mathbf{x}_s, \\ 0, & \mathbf{x}_t \not\subseteq_{\text{UM}} \mathbf{x}_s, \end{cases} \quad (\text{D.1})$$

where $\mathbf{x}_t \subseteq_{\text{UM}} \mathbf{x}_s$ denotes $\forall i : x_t^i \neq [\mathbf{M}]$, we have $\mathbf{x}_t^i = \mathbf{x}_s^i$.

Proof. Using Bayes' theorem, $p_{s|t}(\mathbf{x}_s | \mathbf{x}_t) = p_{t|s}(\mathbf{x}_t | \mathbf{x}_s) \frac{p_s(\mathbf{x}_s)}{p_t(\mathbf{x}_t)}$.

From Proposition 1:

$$p_t(\mathbf{x}_t) = [1 - e^{-\bar{\sigma}(t)}]^{d_1} [e^{-\bar{\sigma}(t)}]^{d_2} p_0(\mathbf{x}_t^{\text{UM}}), \quad (\text{D.2})$$

$$p_s(\mathbf{x}_s) = [1 - e^{-\bar{\sigma}(s)}]^{d_1 - \Delta d} [e^{-\bar{\sigma}(s)}]^{d_2 + \Delta d} p_0(\mathbf{x}_s^{\text{UM}}). \quad (\text{D.3})$$

Utilizing Eq. (B.12), we get

$$p_{t|s}(\mathbf{x}_t | \mathbf{x}_s) = \prod_{i=1}^d p_{t|s}^i(x_t^i | x_s^i) = \begin{cases} [e^{-(\bar{\sigma}(t) - \bar{\sigma}(s))}]^{d_2} [1 - e^{-(\bar{\sigma}(t) - \bar{\sigma}(s))}]^{\Delta d}, & \mathbf{x}_t \subseteq_{\text{UM}} \mathbf{x}_s, \\ 0, & \mathbf{x}_t \not\subseteq_{\text{UM}} \mathbf{x}_s. \end{cases} \quad (\text{D.4})$$

Simplifying these equations, we can express $p_{s|t}(\mathbf{x}_s|\mathbf{x}_t)$ as

$$p_{s|t}(\mathbf{x}_s|\mathbf{x}_t) = \begin{cases} \left[\frac{e^{-\bar{\sigma}(s)} - e^{-\bar{\sigma}(t)}}{1 - e^{-\bar{\sigma}(s)}} \right]^{\Delta d} \left[\frac{1 - e^{-\bar{\sigma}(s)}}{1 - e^{-\bar{\sigma}(t)}} \right]^{d_1} \frac{p_0(\mathbf{x}_s^{\text{UM}})}{p_0(\mathbf{x}_t^{\text{UM}})}, & \mathbf{x}_t \subseteq_{\text{UM}} \mathbf{x}_s, \\ 0, & \mathbf{x}_t \not\subseteq_{\text{UM}} \mathbf{x}_s. \end{cases} \quad (\text{D.5})$$

□

It should be noted that when $\mathbf{x}_t \subseteq_{\text{UM}} \mathbf{x}_s$, the ratio $\frac{p_0(\mathbf{x}_s^{\text{UM}})}{p_0(\mathbf{x}_t^{\text{UM}})}$ can be reformulated as a d_1 -dimensional conditional distribution $p_0(\mathbf{x}_s^{\text{UM}}|\mathbf{x}_t^{\text{UM}})$ with N^{d_1} states. This is not accessible using our one-dimensional conditional distribution $p_0(\hat{x}_t^i|\mathbf{x}_t^{\text{UM}})$ in Theorem 1 if $d_1 > 1$. Therefore, for efficiency, existing samplers assume that each dimension is independent within a small interval and update each dimension in parallel [29, 26].

D.2 Tweedie τ -leaping method and its simplified form in RADD

Given the vector \mathbf{x}_t , if we sample each x_s^i independently, the factorization of marginal distribution $p_{s|t}^{\text{tweedie}}$ results in the minimum KL divergence with true reverse $p_{s|t}(\mathbf{x}_s|\mathbf{x}_t)$ (proof in [29], Appendix A). This assumption formally defines $p_{s|t}^{\text{tweedie}}$ as follows:

$$p_{s|t}^{\text{tweedie}}(\mathbf{x}_s|\mathbf{x}_t) = \prod_{i=1}^d p_{s|t}^{\text{tweedie},i}(x_s^i|\mathbf{x}_t) = \prod_{i=1}^d p_{s|t}^i(x_s^i|\mathbf{x}_t). \quad (\text{D.6})$$

To sample from $p_{s|t}^{\text{tweedie}}$, we need to derive the analytic form of $p_{s|t}^i(x_s^i|\mathbf{x}_t)$. Without loss of generality, let's assume that the preceding d_1 terms of \mathbf{x}_t are all $[\mathbf{M}]$, and the remaining d_2 terms are unmasked tokens.

For illustration, we can take $i = 1$ as an example. Let $\tilde{\mathcal{X}}_k$ denote the sample space of length $d_1 - 1$ sequence where each sequence has exact k masked tokens, with $|\tilde{\mathcal{X}}_k| = C_{d_1-1}^k N^{d_1-1-k}$. When $x_s^1 \neq [\mathbf{M}]$, According to Lemma 2:

$$\begin{aligned} p_{s|t}^1(x_s^1|\mathbf{x}_t) &= \sum_{\mathbf{x}_s^{2:d}} p_{s|t}(\mathbf{x}_s|\mathbf{x}_t) \\ &= \sum_{k=0}^{d_1-1} \sum_{\mathbf{x}_s^{2:d} \in \tilde{\mathcal{X}}_k} \left[\frac{e^{-\bar{\sigma}(s)} - e^{-\bar{\sigma}(t)}}{1 - e^{-\bar{\sigma}(s)}} \right]^{k+1} \left[\frac{1 - e^{-\bar{\sigma}(s)}}{1 - e^{-\bar{\sigma}(t)}} \right]^{d_1} \frac{p_0(x_s^1, \mathbf{x}_s^{2:d, \text{UM}}, \mathbf{x}_t^{d_1+1:d})}{p_0(\mathbf{x}_t^{d_1+1:d})} \\ &= \sum_{k=0}^{d_1-1} C_{d_1-1}^k \left[\frac{e^{-\bar{\sigma}(s)} - e^{-\bar{\sigma}(t)}}{1 - e^{-\bar{\sigma}(s)}} \right]^{k+1} \left[\frac{1 - e^{-\bar{\sigma}(s)}}{1 - e^{-\bar{\sigma}(t)}} \right]^{d_1} \frac{p_0(x_s^1, \mathbf{x}_t^{d_1+1:d})}{p_0(\mathbf{x}_t^{d_1+1:d})} \\ &= \frac{e^{-\bar{\sigma}(s)} - e^{-\bar{\sigma}(t)}}{1 - e^{-\bar{\sigma}(s)}} \left[1 + \frac{e^{-\bar{\sigma}(s)} - e^{-\bar{\sigma}(t)}}{1 - e^{-\bar{\sigma}(s)}} \right]^{d_1-1} \left[\frac{1 - e^{-\bar{\sigma}(s)}}{1 - e^{-\bar{\sigma}(t)}} \right]^{d_1} \frac{p_0(x_s^1, \mathbf{x}_t^{d_1+1:d})}{p_0(\mathbf{x}_t^{d_1+1:d})} \\ &= \frac{e^{-\bar{\sigma}(s)} - e^{-\bar{\sigma}(t)}}{1 - e^{-\bar{\sigma}(t)}} \frac{p_0(x_s^1, \mathbf{x}_t^{d_1+1:d})}{p_0(\mathbf{x}_t^{d_1+1:d})} \\ &= \frac{e^{-\bar{\sigma}(s)} - e^{-\bar{\sigma}(t)}}{1 - e^{-\bar{\sigma}(t)}} p_0(x_s^1|\mathbf{x}_t^{d_1+1:d}). \end{aligned}$$

Here, we used the binomial expansion identity:

$$\sum_{k=0}^{d_1-1} C_{d_1-1}^k \left[\frac{e^{-\bar{\sigma}(s)} - e^{-\bar{\sigma}(t)}}{1 - e^{-\bar{\sigma}(s)}} \right]^k = \left[1 + \frac{e^{-\bar{\sigma}(s)} - e^{-\bar{\sigma}(t)}}{1 - e^{-\bar{\sigma}(s)}} \right]^{d_1-1}.$$

Similarly, for $x_s^1 = [\mathbf{M}]$:

$$p_{s|t}^1([\mathbf{M}]|\mathbf{x}_t) = \frac{1 - e^{-\bar{\sigma}(s)}}{1 - e^{-\bar{\sigma}(t)}}. \quad (\text{D.7})$$

In general, we have

$$p_{s|t}^i(x_s^i|\mathbf{x}_t) = \begin{cases} \frac{e^{-\bar{\sigma}(s)} - e^{-\bar{\sigma}(t)}}{1 - e^{-\bar{\sigma}(t)}} p_0(x_s^i|\mathbf{x}_t^{\text{UM}}), & x_s^i \neq [\mathbf{M}], x_t^i = [\mathbf{M}], \\ \frac{1 - e^{-\bar{\sigma}(s)}}{1 - e^{-\bar{\sigma}(t)}}, & x_s^i = [\mathbf{M}], x_t^i = [\mathbf{M}], \\ \delta_{x_s^i x_t^i}, & x_t^i \neq [\mathbf{M}]. \end{cases} \quad (\text{D.8})$$

With trained \mathbf{c}_θ , we can use $\mathbf{c}_\theta(\mathbf{x}_t)[i, x_s^i]$ to approximate the true conditional distribution $p_0(x_s^i|\mathbf{x}_t^{\text{UM}})$ and sample by Eq. (D.8).

D.3 Euler method and its simplified form in RADD

According to theory of CTMC [35, 26, 29], given a particular one-dimensional input x_t , the transition probabilities to x_s can be approximately calculated using Eq. (2.1) and Eq. (2.7) as follows:

$$p_{s|t}(x_s|x_t) = \delta_{x_t x_s} + \tilde{\mathbf{Q}}_t(x_t, x_s)(t-s) + o(t-s), \quad (\text{D.9})$$

$$\approx \delta_{x_t x_s} + \tilde{\mathbf{Q}}_t(x_t, x_s)(t-s), \quad (\text{D.10})$$

where

$$\tilde{\mathbf{Q}}_t(x_t, x_s) = \begin{cases} \mathbf{Q}_t(x_s, x_t) \frac{p_t(x_s)}{p_t(x_t)}, & x_t \neq x_s, \\ -\sum_{k \neq x_t} \mathbf{Q}_t(x_t, k), & x_t = x_s. \end{cases} \quad (\text{D.11})$$

Therefore, we can define the Euler approximation of the transition probability [26, 29]:

$$p_{s|t}^{\text{euler}}(x_s|x_t) = \delta_{x_t x_s} + \tilde{\mathbf{Q}}_t(x_t, x_s)(t-s) \quad (\text{D.12})$$

For multi-dimensional case, we factorize $p_{s|t}^{\text{euler}}(\mathbf{x}_s|\mathbf{x}_t)$ as $\prod_{i=1}^d p_{s|t}^{\text{euler},i}(x_s^i|\mathbf{x}_t)$, where $p_{s|t}^{\text{euler},i}(x_s^i|\mathbf{x}_t)$ is based on Eq. (D.12) which use \mathbf{x}_t to replace x_t and $x_t^1 \cdots x_s^i \cdots x_t^d$ to replace x_s .

In the case of absorbing diffusion, similar to Tweedie- τ leaping method in Appendix D.2, we can use Theorem 1 and Eq. (2.4) to simplify Eq. (D.12), which results in

$$p_{s|t}^{\text{euler},i}(x_s^i|\mathbf{x}_t) = \begin{cases} \sigma(t) \frac{e^{-\bar{\sigma}(t)}}{1 - e^{-\bar{\sigma}(t)}} (t-s) p_0(x_s^i|\mathbf{x}_t^{\text{UM}}), & \text{if } x_s^i \neq [\mathbf{M}], x_t^i = [\mathbf{M}] \\ 1 - \sigma(t) \frac{e^{-\bar{\sigma}(t)}}{1 - e^{-\bar{\sigma}(t)}} (t-s), & \text{if } x_s^i = [\mathbf{M}], x_t^i = [\mathbf{M}] \\ \delta_{x_s^i x_t^i}, & x_t^i \neq [\mathbf{M}]. \end{cases} \quad (\text{D.13})$$

In practice, we also use $\mathbf{c}_\theta(\mathbf{x}_t)[i, x_s^i]$ to approximate the true conditional distribution $p_0(x_s^i|\mathbf{x}_t^{\text{UM}})$ when sampling from Eq. (D.13).

D.4 Equivalence of Tweedie τ -leaping and Euler method under log-linear noise schedule

By comparing Eq. (D.8) and Eq. (D.13), we observe that both the Tweedie τ -leaping and Euler methods can be interpreted similarly:

- If x_t^i is an unmasked token, keep it unchanged, i.e., $x_s^i = x_t^i$.
- If x_t^i is a masked token, first determine whether it will be unmasked with a probability $\psi(t, s)$. If it is to be unmasked, then sample x_s^i from $p_0(x_s^i|\mathbf{x}_t^{\text{UM}})$.

The only difference lies in the analytic form of $\psi(t, s)$. For the two methods, according to Eqs. (D.8) and (D.13), their corresponding $\psi(t, s)$ are given as follows:

$$\psi^{\text{tweedie}}(t, s) = \frac{e^{-\bar{\sigma}(s)} - e^{-\bar{\sigma}(t)}}{1 - e^{-\bar{\sigma}(t)}}, \quad (\text{D.14})$$

$$\psi^{\text{euler}}(t, s) = \sigma(t) \frac{e^{-\bar{\sigma}(t)}}{1 - e^{-\bar{\sigma}(t)}} (t-s). \quad (\text{D.15})$$

In general cases, these two expressions are not equivalent. However, if we choose a log-linear noise schedule $\bar{\sigma}(t) = 1 - \log(1 - (1 - \epsilon)t)$, both Eq. (D.15) and Eq. (D.14) can be simplified to the same form $\psi(t, s)$ as follows:

$$\psi(t, s) = \frac{t-s}{t}, \quad (\text{D.16})$$

which shows that these two sampling methods are equivalent under a log-linear noise schedule.

D.5 Discuss on the expectation of NFEs

In this part, we show that given the noise schedule $\sigma(t)$ and a set of time steps $\{t_0 = 0, \dots, t_n = T\}$, the NFEs can be treated as a random variable with a calculable expected value for both Euler method and Tweedie τ -leaping method.

Let l denote the length of the generated sequence and $N_k \in \{0, \dots, l\}$ denote the number of dimensions that \mathbf{x} changed in $[t_{k-1}, t_k)$. Without loss of generality, we first consider the unconditional generation case where $l = d$. The NFEs, E-NFEs, and N_k can be expressed as

$$\text{NFEs}(n) = \sum_{k=1}^n \mathbb{I}(N_k \neq 0), \quad (\text{D.17})$$

$$\text{E-NFEs}(n) = \sum_{k=1}^n \mathbb{E}[\mathbb{I}(N_k \neq 0)] = \sum_{k=1}^n P(N_k \neq 0), \quad (\text{D.18})$$

$$N_k = \sum_{i=1}^d \mathbb{I}(x_{t_{k-1}}^i \neq [\mathbf{M}], x_{t_k}^i = [\mathbf{M}]). \quad (\text{D.19})$$

Furthermore, we note that the d dimensions are independent. According to Eqs. (D.8) and (D.13), the probability $p_{s|t}^{i,i}([\mathbf{M}]|\mathbf{x}_t)$ depends only on time and x_t^i while independent of the other dimensions of \mathbf{x}_t . Thus, $p_{s|t}^{i,i}([\mathbf{M}]|\mathbf{x}_t) = p_{s|t}^{i,i}([\mathbf{M}]|x_t^i)$. Therefore, whether a token changes from masked to unmasked is independent across the d dimensions⁴:

$$p(\mathbb{I}(x_s^1 = [\mathbf{M}]), \dots, \mathbb{I}(x_s^d = [\mathbf{M}]) | \mathbb{I}(x_t^1 = [\mathbf{M}]), \dots, \mathbb{I}(x_t^d = [\mathbf{M}])) \quad (\text{D.20})$$

$$= \prod_{i=1}^d p(\mathbb{I}(x_s^i = [\mathbf{M}]) | \mathbb{I}(x_t^i = [\mathbf{M}])). \quad (\text{D.21})$$

Since \mathbf{x}_T consists entirely of masked tokens with probability one, each dimension of $\mathbb{I}(x_{t_{k-1}}^i \neq [\mathbf{M}], x_{t_k}^i = [\mathbf{M}])$ is independent. Consequently, N_k follows a binomial distribution with parameters d and r_k , denoted as $N_k \sim \text{Binomial}(d, r_k)$, where $r_k = p(x_{t_{k-1}}^i \neq [\mathbf{M}], x_{t_k}^i = [\mathbf{M}])$ represents the probability that x^i changes within the interval $[t_{k-1}, t_k)$ in each dimension. Therefore, we can further simplify Eq. (D.18):

$$\text{E-NFEs}(n) = \sum_{k=1}^n P(N_k \neq 0) = \sum_{k=1}^n (1 - (1 - r_k)^d). \quad (\text{D.22})$$

By definition of r_k and property of absorbing diffusion:

$$r_k = p(x_{t_{k-1}}^i \neq [\mathbf{M}], x_{t_k}^i = [\mathbf{M}]) \quad (\text{D.23})$$

$$= p(x_{t_{k-1}}^i \neq [\mathbf{M}] | x_{t_k}^i = [\mathbf{M}]) \prod_{j=k+1}^n p(x_{t_{j-1}}^i = [\mathbf{M}] | x_{t_j}^i = [\mathbf{M}]) p(x_{t_n}^i = [\mathbf{M}]) \quad (\text{D.24})$$

$$= \left(1 - p(x_{t_{k-1}}^i = [\mathbf{M}] | x_{t_k}^i = [\mathbf{M}])\right) \prod_{j=k+1}^n p(x_{t_{j-1}}^i = [\mathbf{M}] | x_{t_j}^i = [\mathbf{M}]). \quad (\text{D.25})$$

Eq. (D.25) can be determined given the sampling method and noise schedule.

For Tweedie τ -leaping, based on Eq. (D.8), we can derive that:

$$p(x_{t_{j-1}}^i = [\mathbf{M}] | x_{t_j}^i = [\mathbf{M}]) = \frac{1 - e^{-\bar{\sigma}(t_{j-1})}}{1 - e^{-\bar{\sigma}(t_j)}}. \quad (\text{D.26})$$

Therefore, we can express r_k as

⁴The independence applies to whether a token changes from masked to unmasked. However, the specific unmasked token a masked token changes to depends on other dimensions.

$$r_k = \left(\frac{e^{-\bar{\sigma}(t_{k-1})} - e^{-\bar{\sigma}(t_k)}}{1 - e^{-\bar{\sigma}(t_k)}} \right) \prod_{j=k+1}^n \left(1 - \frac{1 - e^{-\bar{\sigma}(t_{j-1})}}{1 - e^{-\bar{\sigma}(t_j)}} \right) = \frac{e^{-\bar{\sigma}(t_{k-1})} - e^{-\bar{\sigma}(t_k)}}{1 - e^{-\bar{\sigma}(t_n)}}. \quad (\text{D.27})$$

For the Euler method, based on Eq. (D.13), we can derive that:

$$p(x_{t_{j-1}}^i = [\mathbf{M}] | x_{t_j}^i = [\mathbf{M}]) = 1 - \sigma(t_j) \frac{e^{-\bar{\sigma}(t_j)}}{1 - e^{-\bar{\sigma}(t_j)}} (t_j - t_{j-1}). \quad (\text{D.28})$$

$$r_k = \left(\sigma(t_k) \frac{e^{-\bar{\sigma}(t_k)}}{1 - e^{-\bar{\sigma}(t_k)}} (t_k - t_{k-1}) \right) \prod_{j=k+1}^n \left(1 - \sigma(t_j) \frac{e^{-\bar{\sigma}(t_j)}}{1 - e^{-\bar{\sigma}(t_j)}} (t_j - t_{j-1}) \right). \quad (\text{D.29})$$

For conditional generation cases where the generating sequence length l is less than the dimension d , similar results hold. The only difference is that $N_k \sim \text{Binomial}(l, r_k)$ and Eq. (D.22) changes to

$$\text{E-NFEs}(n) = \sum_{k=1}^n (1 - (1 - r_k)^l). \quad (\text{D.30})$$

Specifically, if we adopt a log-linear noise schedule and let $t_k = \frac{k}{n}$, according to Appendix D.4, the Euler method and Tweedie τ -leaping method are equivalent. In this case, Eq. (D.27) simplifies to $\frac{1}{n}$. Substituting this result into Eq. (D.22), we obtain

$$\text{E-NFEs}(n) = \sum_{k=1}^n (1 - (1 - \frac{1}{n})^l) = n(1 - (1 - \frac{1}{n})^l). \quad (\text{D.31})$$

E Discussion for mean parameterization and RADD

Equivalence of modeling Analogous to the x_0 prediction in continuous state diffusion models, Austin et al. [20] and Campbell et al. [26] used the mean parameterization $\mu_\theta(x_t, t)$ to learn the reverse density $p_{0|t}^i(x_0^i | x_t)$, $i = 1 \cdots d$. According to the analytic form of reverse distribution in Eq. (D.8), letting $s = 0$, we have:

$$p_{0|t}^i(x_0^i | x_t) = \begin{cases} p_0(x_0^i | x_t^{\text{UM}}), & x_0^i \neq [\mathbf{M}], x_t^i = [\mathbf{M}], \\ 0, & x_0^i = [\mathbf{M}], x_t^i = [\mathbf{M}], \\ \delta_{x_0^i x_t^i}, & x_0^i \neq [\mathbf{M}]. \end{cases} \quad (\text{E.1})$$

This shows that the mean prediction is equivalent to learning conditional distributions on clean data. In conjunction with our discussion in Section 3.1, the mean parameterization should be time-independent, denoted as $\mu_\theta(x_t)$, and is equivalent to our reparameterized $c_\theta(x_t)$. Empirical results He et al. [25] and Sahoo et al. [47], which demonstrate that the time-independent model $\mu_\theta(x_t)$ performs well, also validate our theory.

Equivalence of training objectives Shi et al. [42] proved that the training loss for score parameterization (i.e., DSE loss) and mean parameterization (i.e., negative ELBO loss) is equivalent.

Equivalence of sampling methods Comparing our Appendix D.2 with Shi et al. [42], Sahoo et al. [47], it is evident that the Tweedie τ -leaping method for score parameterization is equivalent to the sampling method for mean prediction as follows:

$$q_\theta(x_s | x_t) = p(x_s | x_t, x_0 = \mu(x_t)) = \begin{cases} \text{Cat}(x_s; x_t), & x_t \neq [\mathbf{M}], \\ \text{Cat}(x_s; \frac{1-\alpha_s}{1-\alpha_t} \mathbf{e}_{[\mathbf{M}]} + \frac{\alpha_s - \alpha_t}{1-\alpha_t} \mu(x_t)), & x_t = [\mathbf{M}]. \end{cases} \quad (\text{E.2})$$

Here, α_t represents the probability of a token remaining unmasked at time t , which equals $e^{-\bar{\sigma}(t)}$ for score parameterization. Therefore, Eq. (E.2) and Eq. (D.8) is equivalent.

F Algorithms for training and sampling

Algorithm 1 Unconditional Sampling

Require: Network \mathbf{c}_θ , noise schedule σ , time range $[0, T]$, step size Δt

$t \leftarrow T$, $\mathbf{x}_T \leftarrow [\mathbf{M}] \dots [\mathbf{M}]$, $\mathbf{c}_{cache} \leftarrow \mathbf{c}_\theta(\mathbf{x}_t)$.

while $t > 0$ **do**

if Use Euler **then**

 Construct transition densities $p_{t-\Delta t|t}^{\text{euler},i}(x_{t-\Delta t}^i|\mathbf{x}_t)$ by Eq. (D.13) with \mathbf{c}_{cache} .

$x_{t-\Delta t}^i \sim \text{Cat}(p_{t-\Delta t|t}^{\text{euler},i}(x_{t-\Delta t}^i|\mathbf{x}_t))$ for all $x_t^i = [\mathbf{M}]$, $x_{t-\Delta t}^i \leftarrow x_t^i$ for all $x_t^i \neq [\mathbf{M}]$.

end if

if Use Tweedie τ -leaping **then**

 Construct transition densities $p_{t-\Delta t|t}^i(x_{t-\Delta t}^i|\mathbf{x}_t)$ by Eq. (D.8) with \mathbf{c}_{cache} .

$x_{t-\Delta t}^i \sim \text{Cat}(p_{t-\Delta t|t}^i(x_{t-\Delta t}^i|\mathbf{x}_t))$ for all $x_t^i = [\mathbf{M}]$, $x_{t-\Delta t}^i \leftarrow x_t^i$ for all $x_t^i \neq [\mathbf{M}]$.

end if

if $\mathbf{x}_{t-\Delta t} \neq \mathbf{x}_t$ **then**

$\mathbf{c}_{cache} \leftarrow \mathbf{c}_\theta(\mathbf{x}_t)$.

end if

$t \leftarrow t - \Delta t$.

end while

Algorithm 2 Conditional Sampling

Require: Network \mathbf{c}_θ , noise schedule σ , time $[0, T]$, step size Δt , Prompt spaces Ω and tokens \mathcal{T} .

$t \leftarrow T$, construct \mathbf{x}_T with $\mathbf{x}_T^\Omega = \mathcal{T}$ and $\mathbf{x}_T^\Omega = [\mathbf{M}]$, $\mathbf{c}_{cache} \leftarrow \mathbf{c}_\theta(\mathbf{x}_t)$.

while $t > 0$ **do**

if Use Euler **then**

 Construct transition densities $p_{t-\Delta t|t}^{\text{euler},i}(x_{t-\Delta t}^i|\mathbf{x}_t)$ by Eq. (D.13) with \mathbf{c}_{cache} .

$x_{t-\Delta t}^i \sim \text{Cat}(p_{t-\Delta t|t}^{\text{euler},i}(x_{t-\Delta t}^i|\mathbf{x}_t))$ for all $x_t^i = [\mathbf{M}]$, $x_{t-\Delta t}^i \leftarrow x_t^i$ for all $x_t^i \neq [\mathbf{M}]$.

end if

if Use Tweedie τ -leaping **then**

 Construct transition densities $p_{t-\Delta t|t}^i(x_{t-\Delta t}^i|\mathbf{x}_t)$ by Eq. (D.8) with \mathbf{c}_{cache} .

$x_{t-\Delta t}^i \sim \text{Cat}(p_{t-\Delta t|t}^i(x_{t-\Delta t}^i|\mathbf{x}_t))$ for all $x_t^i = [\mathbf{M}]$, $x_{t-\Delta t}^i \leftarrow x_t^i$ for all $x_t^i \neq [\mathbf{M}]$.

end if

if $\mathbf{x}_{t-\Delta t} \neq \mathbf{x}_t$ **then**

$\mathbf{c}_{cache} \leftarrow \mathbf{c}_\theta(\mathbf{x}_t)$.

end if

$t \leftarrow t - \Delta t$.

end while

Algorithm 3 Training (t -DCE Loss)

Require: Network \mathbf{c}_θ , noise schedule σ , time $[0, T]$, samples from data distribution p_{data}

repeat

$\mathbf{x}_0 \sim p_{\text{data}}$, $t \sim U([0, T])$.

 Construct \mathbf{x}_t by $\xi^i \sim \text{Bernoulli}(e^{-\sigma(t)})$, $x_t^i = \mathbb{I}(\xi^i = 1)x_0^i + \mathbb{I}(\xi^i = 0)[\mathbf{M}]$.

 Calculate $L_\theta(\mathbf{x}_t, \mathbf{x}_0) = \sum_{x_t^i = [\mathbf{M}]} -\sigma(t) \frac{e^{-\sigma(t)}}{1-e^{-\sigma(t)}} \log \left(\frac{e^{-\sigma(t)}}{1-e^{-\sigma(t)}} \mathbf{c}_\theta(\mathbf{x}_t)[i, x_0^i] \right)$.

 Calculate $\nabla_\theta L(\mathbf{x}_t, \mathbf{x}_0)$ and run optimizer.

until converged

Algorithm 4 Training (λ -DCE Loss)

Require: Network c_θ , samples from data distribution p_{data}

repeat

$x_0 \sim p_{\text{data}}, \lambda \sim U([0, 1]).$

Construct x_λ by $\xi^i \sim \text{Bernoulli}(1 - \lambda), x_\lambda^i = \mathbb{I}(\xi^i = 1)x_0^i + \mathbb{I}(\xi^i = 0)[\mathbf{M}].$

Calculate $L_\theta(x_\lambda, x_0) = \sum_{x_\lambda^i = [\mathbf{M}]} -\frac{1}{\lambda} \log(c_\theta(x_\lambda)[i, x_0^i]).$

Calculate $\nabla_\theta L(x_\lambda, x_0)$ and run optimizer.

until converged

G Experimental details

G.1 Model details

We implemented our RADD model based on the SEDD architecture, an encoder-only transformer model [53, 54]. Our model incorporates rotary positional encoding [55] but excludes all parts related to time conditioning (i.e., TimeEmbedding, adaLN-zero block [56]). Instead, we added a softmax operation at the end of the neural network to ensure the output is a valid conditional distribution. Our modification resulted in a reduction of 7 million parameters, leading to an 8% decrease from the original 90 million non-embedding parameters of the SEDD small model.

G.2 Training details

We trained our RADD-DSE model following the configuration settings from [29]. The training configuration is as follows:

- Batch Size: 512
- Learning Rate: 3×10^{-4}
- Exponential Moving Average (EMA): 0.9999
- Gradient Clipping: Gradient norm clipped to 1
- Warmup Schedule: Applied for the first 2500 iterations
- weight decay: 0
- dropout rate: 0.1

For the models RADD- t -DCE, RADD- λ -DCE, and RADD-AO, we referenced the hyperparameters from [42]. The modifications included setting the weight decay to 0.03 and the dropout rate to 0.02. Due to limited computational resources, we did not conduct a hyperparameter search and ran experiments directly with these configurations. Further hyperparameter tuning may improve performance.

We trained on nodes of 32 V100 32G GPUs with float16 precision.

G.3 Unconditional Generation Details

For unconditional generation, we employed a log-linear noise schedule. As illustrated in Section 3.2, the Euler method and the Tweedie τ -leaping method are equivalent under this case. In practice, the implementation of the Euler method and the Tweedie τ -leaping method remains the same for RADD but differs for SEDD. So we measure the perplexity of SEDD by Tweedie τ -leaping method which performs slightly better while it suffices to measure the perplexity of RADD once.

The following procedures were used for generating samples:

- RADD Small: We generated 1024 samples to calculate the average value.
- SEDD Small: We utilized the results provided for steps less than 2048 and performed our evaluation at 4096 steps.

No annealing methods (e.g., top-p or top-k sampling) were applied in our sampling process.

G.4 Further evaluation of generative perplexity

Runtime Comparison To assess inference efficiency, we measured the inference time on a single NVIDIA 4090 GPU with a batch size of 8, averaged over 1024 samples. The results are summarized in Table 3.

Across all sampling steps, the RADD model consistently required the shortest sampling time while maintaining similar perplexity levels to the SEDD model. Quantitatively, RADD achieved a speed-up of 2.5 to 3.5 times, as shown in Table 3. These findings align with the analysis of the E-NFEs in Fig. 1, validating the effectiveness of the RADD model and the caching strategy. They also demonstrate the practical implications of our Theorem 1.

Table 3: **Average inference time per sample with varying sampling steps.** The table compares the average inference time (in seconds) for the SEDD small model using both Euler and Tweedie τ -leaping (T- τ) sampling methods, and the RADD small model under a log-linear noise schedule with a caching strategy.

Methods	Metrics	32	64	128	256	512	1024	2048	4096
SEDD (euler)	Time(s)	0.48	0.87	1.67	3.25	6.41	12.74	25.42	50.86
	PPL	155	105	81	66	53	43	35	28
SEDD (T- τ)	Time(s)	0.38	0.68	1.28	2.47	4.85	9.61	19.14	38.20
	PPL	151	104	81	65	52	42	34	28
RADD (cache)	Time(s)	0.33	0.54	0.94	1.68	2.97	5.15	8.73	14.88
	PPL	158	110	83	67	54	44	35	28

Sampling as any-order autoregressive models As outlined in Theorem 1, c_θ can be interpreted as a conditional distribution over clean data. One natural approach is to use this directly for generating samples, similar to any-order autoregressive models. However, there are $d!$ possible ways to decompose the joint distribution into conditional distributions. We tested three representative cases:

- forward: $p(x^1 \cdots x^d) = \prod_{k=1}^d p(x^k | x^{(<k)})$
- backward: $p(x^1 \cdots x^d) = \prod_{k=1}^d p(x^k | x^{(>k)})$
- random: $\pi \sim U_\pi, p(x^1 \cdots x^d) = \prod_{k=1}^d p(x^{\pi(k)} | x^{\pi(<k)})$

The results are presented in Table 4. Perplexity was calculated as the average over 1024 samples. For the random case, we calculated the average perplexity across different randomly generated π . Generally, we found that directly sampling from the conditional distribution resulted in higher perplexity compared to Tweedie τ -leaping or the Euler method with similar computational costs. Among the different decomposition orders, the forward order demonstrated the best performance.

Table 4: **Quality of unconditionally generated text evaluated by perplexity (\downarrow).** For a fixed model, the best perplexity is **bolded**.

Method	RADD- t -DCE	RADD- λ -DCE
Forward	102.90	98.07
Backward	118.86	113.56
Random	108.11	111.02

H Additional experimental results

H.1 Additional samples

Additional unconditionally and conditionally generated text of RADD- t -DCE and RADD- λ -DCE are reported in Figs. 3 to 6. All samples are generated with 1024 steps under a log-linear noise schedule.

case feature — NBC is making this year the second season of the show — in addition, would include the Sesame Street Family, where a son is given to him and Sara, Tamina, Rh June. Haley didn't learn from as accurately as she had anticipated.

"You kind of had Harmon known — 'trust us, we're going to hear the future of the show as well...' But you didn't know what their plan is and then get back to it," Harmon said. "The producers found themselves put together stories that were very complicated for me to get a plan about."

Rhodes Harmon has stated that Tamina is part of the show's legacy, and had a half known how much tidings flowed about Sara's development. So, she wouldn't get too much chance to play as Sara and Tamina in the family that is currently intact.

"I was very excited with what I saw," she said. "Usually it never tried to be a commercial... often it was just a very side show. I thought I had something in Fortune but hadn't thought of in a while, and it was a big opportunity."

"Tara is a wonderful guy, and great," she continued. "It was a little weird that I was thinking that everything, his little things, will be important, but if he did it to prompt the fan base to say, like, Tamina would have been good for her, but then the whole family would have been good for her? I love it. You know, she wants something beyond your radar and it's a huge puzzle right now that Tamina and the characters will travel as well if anything bad happens."

The documentary Roots is produced at the BBC1 Family Store March 7, in Los Angeles. Another post-decade question about whether or not her husband is going to be the show's father is completely unknown, but Harmon said say it's time for season's last special episode, The Taste for Truth, at the end of the year and watch with a twist in the show's season finale.

The possibility is closed that the show's music program is on only Sunday nights through October, which is not the point that will soon be reset.

The big point, "either call it," said, is Harmon is still the character of Rh June, and that nobody in the family had expected this character to show up on time because of the television series.

"It's a major shift in the show's run," Harmon crowed. "He has got the level of enthusiasm that he will have on the rest of the show and it's because of the lasting relationship that Steve and I have always spoken about, we are parents and grandparents."

She's still waiting to "when we were going to get this up together," she said. "On Friday, we had the first primetime premiere for City Haze. We had a chance to look forward to new things. What will be the new focus for the 10 years the main show is largely being decided, but I think the foundation is stronger and expanded."

Workh Harmon doesn't think she'll be part of the conversations from creators and fans about both their place and future if she can't hear roses. "The new Roots material, the first episode in mid-June, looks forward to continually hearing and analyzing feedback and perspectives from fans and creators around the world to better understand what is so significant about the project and the show's future in NBC Family," Harmon said, in a statement from NBC's office.

The same content is cut-and-taped in numerous TV channels, including simul and small-parties, but until traditional TV can be launched in the United States, it would be down on the global audience as the channel has had to push over the past few years as it seeks to become America's largest network by featuring more entertainment, highly marketed and exclusive content for all genres.

Today's launch date is telling because so much saturation was made about the show's impact and concern that it would risk pushing away many of the goals that NBC realized with the original Original Series. Harmon, however, might defend that course. With the first chances, she and NBC will do what they need to to help stabilize its financial means and lead toward its selfconciliation to TV platforms on cable and broadcast platforms.

NOVEMBER 30 2011 eCHANNEL - -X
Workers outside a rally against Obamacare held last Thursday December 30, 2016 in St. Paul St, MN

Figure 3: Unconditionally generated text of RADD-t-DCE.

Hi, my name is iph js. I live in Boise Idaho, offensive to people. I would love to have my wife and old care for me simultaneously, as I was brought up to be with me.

It's an amazing experience! Honestly, I wish they could be a nice lady. Here is a truly lovely world where I missed it to be. A perfect family. Heather and Richard married. They are very lucky. Heather has given birth a baby, and I have been her husband. Over take it, lose Am I.

I have had a problem with this experience for some time. I feel like I cry nearly every day. I almost go to sleep, except I know that my face goes crazy. I have invaded my body with some form of cruelty, based on the presence of a certain gender. Sometimes you choose different women differently because does you think you are treated as equal? In a self-inflicted mistake, I was raped, so from that situation you should probably point more toward me. I wasn't interested in hurting Heather if we were going anywhere.

Let me tell you something... I could not attend Heather Canyon Nationals as comfortably as I did taking my wife's side while skiing. I loved the place and will always do. I miss living on there, so this will not be okay. And I do hope you could do as well. Have a wonderful day.

photo

The baby was about the size of a heart! It was so tiny that I've just read it was going to bring the baby here, so I knew where it was going to come with us. As I saw it, it would be about this size:

We concluded our baby together, and peace! And as Heather began my babyhood, just focus on it now. I time it is something serious I care about. My whole body will show me there! <3

photo

Now for the video, here is a women's side shot, and then I did take a full shot later.<endoftext|>Uncles at high speeds are thrust out from rubble under large plates moving fogboats and water in every direction along the coast and within the ocean. This is called a typhoon effect. The vast majority do it unscientific, probably not because some sort of machine scanner will come across a typhoon in most cases. But just this past the massive quake of 6.225 magnitude struck on Niigata Island near Fukushima Washi in Japan. The customs agency reports a "6. 6, magnitude 6-8 quake" But this event might be different which seamounts fogmail and accumulations 2,700 pounds in every inch of salt in northern Okinawa.

Literont, Professor of M geography at the National Meteorological Institute, predicts that a wave might occur here. He suggests that a compensating flow path will be reached by one wave along the coast rising vertically to around 50 meters (90 feet). The vertical waves will then appear waves of water washing down along the oceanside, northern part of the ocean covered. A so-called typhoon will twincross Japan with wave after waves and merge with the South Pacific to liquefy large bodies of water in the coast, he said on Saturday. This gives an important lesson about the salinity. The "Blumen-loz tsunami" also contains the ancient debris which collapsed and destroyed the ancient tomb while covering the five-by-old wall of the mill.

The National Meteorological Institute, Philaeological Experts Society of Gujarati Barrier Seographers and Surcommunity Recognition Foundation are appealing for special financial support in the area for their current programs. This opportunity teaches the importance of focus on cyclical experience in the present time. We should also be able to learn more about the distinctness of the ocean.

It is very appropriate to graduate the student of the School of Japanese Ocean Scientists and the Xinalhi Hua School of Japan. I want to give thanks for our prayer and for the support for our effort. However, it is neither his nor his average. I just want to write some answers that describe the skills of my student, that are here to spark the discussion and debate among my students and the peers who know the importance of our work. Let's see if you find what you think worthy of the people of the land in question.

The award: This award was firsted by a special grant of the National Academy of Social Sciences, being transferred to the Institute in Macao (available online at 06.04.2017).<endoftext|>For domain which is held by Planet Empire, the mandate of a bot is for raising new asset in order to start new and profitable bots, as such are following on a number of events represented have contacted us: past 7 months. ONLY EVENTS: Evolution, some hate storms [Friday, May 29, 06:01 AM GMT].

In this provides 'nukfall' of the fact that this server can always [operate in continuous-time](#).

Figure 4: **Conditionally generated text of RADD-*t*-DCE.** Prompt tokens are highlighted in blue.

people. Can I say to those, who don't support me, what about you?
 Yeah: That's really tough [for them]. . . . thing like that takes like, three months and eight years.

Q: Growing up in a country that you look up, and you constantly feel like something, that you are out there no one has ever told you to be. This happens at times in the United States. Do you think there you will or will go to be so different?

Yeah: It's weird. Sometimes you see that. Sometimes people say "Shame you mother." And sometimes there is just such a big animal. It's kind of weird. . .

But if you take into account all of the stuff that is there, it's kind of insane. So it's not good how it could go. I think it is really crazy that it might be so strange. I just think the US has a good of people – those are amazing people. There are other people already gone.

Q: Do you find it something you have to understand is why they say you need to be different?

Yeah: Well, I mean, there are experiences that are overrated. It's emotions and stuff, because they aren't so out.

You don't need you as a person to be different. You don't necessarily have to be yourself like other people. People have to teach you a lot of things. Because you can't get off people like people do. And when they become powerful, they have more power, so competition is your thing.

Listen: Not all of it is true. Yeah. Yeah. I'm. Absolutely, going through it.

Q: Hates you have to be a specialist in the Pentagon.

Yeah: It is very, very different people. He's one of my best friends in the military. It is pretty important to him – what he hasn't said isn't meant to be real. He didn't want to be something like that and create either wounds in this world or in his mind about what's going on. What I wanted to say is not to give up, but to try the subject of life.

This stream is produced music by Indiewire.

Klay plays a full show in early July in Phoenix and Los Angeles. It sounds convenient to hear me. If you are stronger, go to it. For more information on broadcasting and what our next evening is now to Uneech, which is another podcast player that will be your earpiece for our interview. Reach out @Maku Independent News and subscribe on iTunes<|endoftext|>WASHINGTON – The White House appears to be "unanimously" ordering FBI Director James Comey to turn over documents under House Senate oversight that experts they have drafted to create a domestic scandal that has reportedly mired two agencies.

A senior Republican lawmaker was asked about whether Comey was able to have the government hand over a document at the president's request and have a congressional inquiry as such. And Director James Clapper responded based on CIA director reports that the documents were reportedly "publicly requested."

Speaking to Fox News: "He is out there on Twitter and drafted his document, he asked, and that has its own element of patriotism and a mystery in it," Clapper replied. "When a rogue document was quickly drafted by the president, it's what went on."

Asked with the Republican senators about Spicer's remarks, the head today of the Senate Board of intelligence said: "We're going to continually look at what's happening. And constantly things goes on."

In his Friday press conference, before opening himself to questions, Clapper appeared to only issue one when it was solely about Russia. He comments DOJ Director Rod Rosenstein "flatly denies allegations that Russian actors meddled in our presidential election." He pointed to a decision media release documents depicting that James Comey ordered for heads of all three agencies to step down after he told Comey he would investigate such matters.

Also speaking to The Washington Post, Clapper wrote on Twitter: "When it goes to your President Trump, the problem is too complex for me, the problem is, there's an entire controversy surrounding the election of President Donald Trump." Clapper said that according to The Washington Times, he has spoken with several American Intelligence's including Vice Chairman Michael Flynn, the Chairman of the Joint Chiefs and the former Director of the Intelligence Committee who gave classified information to Trump.

Russia-intelligence members of the Senate Intelligence Committee, including Clapper, believe they could have handed over classified information to the president even if they hadn't been briefed.

"I suspect when him

Figure 5: Unconditionally generated text of RADD- λ -DCE.

I have a urn I am free to respect. And let you respect that. Join Dr. Submarine in the Arc de thanger home. - Meet a Moscow dealer twice, with Johnny O' (Top Shot Teacher), an ex-Killer, the best-riest detective of his generation. Then meet the face of (Dirty Six), a seasoned (to-day) noob. Innovations: acting, hind, nick presence - scene from 1970 wearing a suit in his classless forties

“The Source of All Information”, a classic movie Hitchcock, is expanding its break massively with both a live and theatrical release.

Treasured by filmmaker Thomas Newby, 76, is produced by Meryl Streep, Loretta Cohen and Anton Bukovid, making a return to Whyte Huy.

They reprise the various 1970 novels from Hitchcock films, including “Sleepless Prince” vs. “Moice” from the “Skergirl” dollhouse where Cary Grant made the infamous Tony Hurt-later-landed rooftops “The Dark Dog in the Pacific Northwest”.

Tuesday’s director, Harold Paul projects Hollywood legend actor Tom Peckerman (Mark Ho), as the series’ Long-Space agent, “His Heart is Subjective” to put the character end.

He is played by historian Scar Samson. Featuring partner, new boss Monica Ringling, whose “The Dangers of Life” serves as the board rewrite of “Heebbles the Pale King” originally written by Lutz.

K-Scout is being directed by Academy Award winning economist Paul Thomard, who directed it from the Eccles Motor. Last year we looked at three of Hitchcock’s finest short films, Almost, Handsome (more recently became a play-action film by John Emery) themed around a tall and handsome star.

Amavi is responsible for the new theatrical releases with reprising production of 1979 classic “” of Good Work”.

The film is directed by Abraham Bidder at the Eryphrome in Toronto and produced by Chris Falkenberg with friends Amavi/Jobby Graff. Falkenberg has an audience of 22,100.

Newby inherited these years earlier in his death on Sept. Indians, this film adaptation shown at a Zadan Brothers movieset and lit on the landscape. Characters from the positive, anamorph sera by Alfred Hitchcock’s famous biographers, stand on display on sets. “The most striking moment of the season is the Dr. Submarine’ lines, taken in only a fraction of a second and dazzling shot” when acting choreographer Fred Tikner tweeted. “Jasper Heinrich is present with both eyes, and every aspect of the visual picked out with the robotic extractor mechanism.

“In one, moving draft, the lead role played elegantly by an David Edwards like ‘Master of Blues II’esque by Christian B. Meyer sports a transparent persona of a given-the-hill cop who instead tries to seduce to have.”

Rewards will be distributed by Parout Films and Time Films.

Producers, Thomas Newby and Blake Titus will work for the plaintiff and those who would themselves, and look at those who devoted Ted Hozzi to his credit. Also includes “Mikael Ginsberg”; Hungry and Captain Sherrod/”Canum Mayor”; Gibraltar by Jason Lindber-Malabon.<|endoftext|>The European Court has raised the matter of using technology such as websites to initiate the censorship standoff on the basis of Russian-American-won Europe that could lead to ongoing civil war over increasingly basic question such as your laptop and the Internet.

The Protect Big Brother is introduced in Quantico in 2006 (Dialogue to Fight Rights in California) by the Italian Social Democratic Party. It was formulated to fulfill public hope and freedom and validate the real concept of freedom to square the democratic concept of press freedom and expression.

Leveraging the the authorities’ surveillance and warning of Fascism’s and allied tendencies in light of witnessing of the directness of the political movements and official mainlines is no easy task.

But the occasion demands the re-evaluation of principles that – in the case of National Security Executive Agency (NSA), NNSA), the only gravest threat to the political party without wasting time with playing or political speech.

Meanwhile is Antonio Kassiano Nuovo put it that, “This is a movement now. Europe’s people should cry for it in the near future. We need representative democracy, of vision for participation and of respect for how important are achieving something economic and possible.

“This requires putting an emphasis on the preservation of the speech and freedom [in a joint framework](#).

Figure 6: **Conditionally generated text of RADD-λ-DCE.** Prompt tokens are highlighted in blue.